Anterior teeth root inclination prediction derived from digital models: A comparative study of plaster study casts and CBCT images

Mahmoud Dastoori
MSc, University College London, 2007
DDS, Ajman University of Science and Technology, 2006

Anterior teeth root inclination prediction derived from digital models: A comparative study of plaster study casts and CBCT images

By

Mahmoud Dastoori

MSc, University College London, 2007
DDS, Ajman University of Science and Technology, 2006

Principal Supervisor:

Professor Athanasios E. Athanasiou

Co-supervisors:

Professor Joseph Bouserhal

Professor Demetrios J. Halazonetis

Presented to the Hamdan Bin Mohammed College of Dental Medicine of
Mohammed Bin Rashid University of Medicine and Health Sciences
in Partial Fulfillment of the Requirements for the Degree of
Master of Science in Orthodontics
2017

ABSTRACT

Anterior teeth root inclination prediction derived from digital models: A comparative study of plaster study casts and CBCT images

Mahmoud Dastoori, DDS, MSc

Supervisors:

Professor Athanasios E. Athanasiou
Professor Joseph Bouserhal
Professor Demetrios J. Halazonetis

Aim:

To assess the accuracy of digital models generated using commercially available software to predict anterior teeth root inclination characteristics and compare the results to relevant data obtained from CBCT images.

Materials and Methods:

Following sample size calculation and after evaluation of inclusion and exclusion criteria, pre-treatment maxillary and mandibular plaster models and the corresponding CBCT scans of 31 patients attending a private orthodontic clinic in Beirut, Lebanon, were randomly selected. The subjects represented both genders (males: 10; females: 21), ranging in age from 12 to 40 years. Plaster models were scanned using the high resolution of an Ortho Insight 3D ™ scanner (Motion View Software, Chattanooga, Tennessee, USA) and CBCT scans were taken using a Kodak 9500 Cone Beam 3D System (Carestream Health, Inc., Rochester, New York, USA). Elaboration of plaster models and CBCT data were performed according to specific technical steps. The Shapiro-Wilk test was used to test normality of measurements per tooth and cross-tabulation to examine the independency between categorical variables. Statistical analysis was performed using χ^2 test of association. If the measurements were

normally distributed, the t-test and ANOVA were used to examine two or more continuous independent variables. In cases of non-normality of measurements, the Mann-Whitney and Kruskal-Wallis tests for multi-comparison of continuous data were employed. To evaluate the reliability and consistency of the investigator, the paired t-test was used. P-value was set as ≤ 0.05 in all statistical analyses. To determine the intra-examiner error of the measurements, records of 5 random patients were selected and all measurements were repeated twice by the author after a two week interval and the correlations computed using intra-class correlation coefficient (ICC).

Results:

The maximum disparity in angle between images derived from digital models and CBCT data was almost 40 degrees (upper left canine). The disparity in upper right canines was similar. The upper and lower canines produced the worst results, followed by the lower lateral incisors. The upper central incisors showed the best results, although the maximum angle of difference exceeds 20 degrees (with the median only around 8 degrees). There was no statistically significant difference in measurements of difference between long axes of the root by using the two methods in each tooth (MDBLAR) according to Angle classification.

Observation of the cases showed that the software frequently estimates angulations leading to overlapping of adjacent roots; a clinically unfeasible situation in the absence of extensive root resorption or root morphology variation. Errors were higher for canines and lower for central incisors. There was no correlation of errors between teeth.

Conclusions:

Root morphology imaging prediction is not a primary function of this software and this study confirmed its limitation as a sole tool in routine clinical applications. At

present these predictions cannot be considered accurate or reliable unless correlated with a radiographic image.

DEDICATION

To my parents, the reason of what I have achieved until now. Thank you for your great support and unconditional love.

To my wife, you have been my inspiration and my soul mate. Your sacrificial care made completion of this work possible.

To my family, friends and colleagues, I am really grateful to have you by my side.

DECLARATION

I declare that the entire content of the thesis is my own work. There is no conflict of interest with any other entity or organization.

Name: Mahmoud Dastoori

Signature:

ACKNOWLEDGMENTS

This study was made possible by the guidance and advice from my supervisors. I wish to express my deepest appreciation and gratitude to:

1. Professor Athanasios E. Athanasiou, Hamdan Bin Mohammed College of Dental Medicine, Mohammed Bin Rashid University of Medicine and Health Sciences, for introducing the topic of this thesis to me and his invaluable assistance in the research. He constantly inspired a spirit of adventure and exploration and made perceptive comments and suggestions in the course of this project.
2. Professor Joseph Bouserhal, St. Joseph University, Lebanon, for his pivotal role in the research for this project in supplying the necessary materials. He was generous with his help and offered continual support and invaluable assistance in guiding me towards achieving my goals.
3. Professor Demetrios J. Halazonetis, National and Kapodistrian University of Athens, Greece, for inducting me into the methodology, for facilitating through his software design a very essential part of this work, and for his helpful and constructive criticism and advice during the work for this project.
4. Associate Professor Amar Hassan, Hamdan Bin Mohammed College of Dental Medicine, Mohammed Bin Rashid University of Medicine and Health Sciences, for sharing his perceptive and illuminating views regarding statistics.

LIST OF TABLES

LIST OF FIGURES

Table of Contents Page

GENERAL PART

1. Introduction

Dental impression is the negative replication of hard and soft tissues in the mouth from which a dental model, a positive reproduction, can be formed (Anusavice, 2003).

Dental impressions have progressed since the 1700s. Philipp Pfaff in 18th century was the first to describe impression-taking techniques (Glenner, 1997). Plaster models have been the gold standard in dental diagnosis and treatment procedures. They are the first and only true 3-dimensional (3D) replication of hard and soft tissues of the mouth (Stewart, 2001). However, they require massive storage capacity and their long-term usefulness is compromised by breakage and degradation.

Approximately 30 years ago, the 3D scanning of dental arches was first introduced for use with computer-aided design (CAD) and computer-aided manufacturing (CAM) technology (Mörmann et al., 1985). Since then, 3D digital model scanners have been increasingly incorporated in orthodontic offices and benchtop scanners can now construct a digital 3D image of maxillary and mandibular arches from existing plaster models or impressions; making them a potential replacement for traditional plaster models. 3D digital models are used for several purposes such as storage, diagnosis and the fabrication of customised appliances.

3D digital model scanning is an indirect imaging technique where the physical plaster model or impression is scanned by a laser scanner and subsequently reconstructed as a digital file. Despite the extra step involved when compared to the cone-beam computed tomography (CBCT), which is a direct imaging technique, digital model scanners are rapidly gaining popularity in many orthodontic practices because they cost less, occupy little space, and require minimum maintenance compared to physical models. Furthermore, the scanners and their digital files provide more convenient access to study models (Leifert et al., 2009).

Digital models may be accurate representations of dental anatomy, but they have the limitation of showing only the crown and occlusal surfaces of the teeth and they cannot show the true size, location, or relationships of the roots of the teeth and other anatomical details unless they are correlated with conventional radiographs (e.g., panoramic, lateral or posterior-anterior cephalometric X-rays) or CBCT imaging.

The Ortho insight 3D ™laser scanner (Motion View Software, Chattanooga, Tennessee, USA) became available in 2012. The scanner uses a robotic table and scanning arms to give three axes of motion and 6 degrees of freedom. The scanner has a maximum scan volume of 4x4x2 inches (Bailey et al., 2013) and has an accuracy of 40-200 microns, depending on the selected resolution. This diagnosis and treatment planning software automatically calculates measurements and can set up a variety of simulations, including roots of the teeth. Root length, morphology and angulations are predicted based on information obtained from the scanned crowns of the teeth using mathematical models. However, there is a paucity of investigations regarding the accuracy and reliability of root morphology predictions derived from this type of software.

2. Literature review

2.1 Tooth anatomy

A tooth has two distinct components, namely crown and root, comprises three different hard tissues, namely enamel, dentine and cementum, and contains one soft tissue, namely the pulp (Hillson, 1996).

Human dentition consists of four types of tooth presenting on both sides of the maxilla and mandible. The collective category of anterior teeth comprises incisors and canines; these are single rooted and have one cusp. In contrast, the premolars have a single buccal cusp, one lingual cusp, and are normally single rooted. While the upper molars exhibit four major cusps and three roots, the lower molars have five cusps and two roots. The multicuspid premolars and molars are collectively termed posterior teeth (Scott and Turner, 1997).

Understanding dental anatomy is essential in order to develop an accurate appreciation of the role of teeth in digestion, appearance, speech and sensory input. A deficiency in the proper functioning of the teeth, usually due to disease such as decay or cavities, can result in a person's health, appearance and nutrition being affected (Rose et al., 1985).

Teeth exhibit two types of morphological variations: those concerning the form of their structures; this structural variation is either present or absent in a specific tooth form in a given population. For tooth crowns, this variation may be exhibited as accessory marginal or occlusal ridges, cingular derivatives and supernumerary cusps. For tooth roots this variation is commonly exhibited as a variation in root numbers, although some morphological variables exhibits significant gender differences (e.g., the canine distal accessory ridge). The majority of these traits show similar frequencies and class frequency distributions for males and females.

An important objective of orthodontic treatment is to achieve proper and stable tooth positions and angulations involving not only the crowns, but also their roots. However, the current methods of clinically monitoring root alignment present certain limitations (Lee et al., 2015).

2.2 Methods of root morphology assessment

The use of imaging has become an almost essential diagnostic adjunct to forming a clinical assessment of any dental patient. The radiographic image, in conjunction with the case history and a clinical examination, constitutes one of the most useful important diagnostic aids utilized by dental practitioners. Various radiographic methods and techniques have been developed and have subsequently progressed, including 2D and 3D imaging.

2.2.1 Intraoral periapical radiographs

Periapical radiography consists of intraoral techniques designed to show the entire tooth and its surrounding structures. Each film usually shows two to four teeth. In this technique detailed information of the tooth is taken by placing film in the oral cavity while the X-rays source is outside the oral cavity (Whaites and Drage, 2013).

The main clinical indications for periapical radiography include:

- Detection of apical lesions
- Detection and evaluation of dental caries
- Assessment of the periodontal status
- Assessment of alveolar bone after traumatic injury to the tooth
- Assessment of the presence and position of unerupted teeth in mixed dentition
- Assessment of root morphology before extractions

- Assessment of pulp pathology
- Assessment during endodontic treatment
- Preoperative assessment and postoperative appraisal of apical surgery
- Detailed evaluation of apical cysts and other lesions within the alveolar bone
- Evaluation of implants postoperatively

The advantages of periapical radiography are:

- Optimum imaging characteristics including density, contrast, definition and detail
- Less distortion; most distortions are caused by improper angulations of X-ray beam
- Actual life size image of same size and shape
- Area of interest should be visible in the X-rays, usually 2-3 mm beyond the apices
- Simple procedure
- No overlapping, and
- No artifacts

Factors affecting accuracy of periapical radiography may include:

- X-rays beam location
- Exposure factor selection, and
- Film placement.

The periapical radiography techniques include:

- Bisecting line angle technique
- Le Master technique
- Parallel line angle technique

Radiation dose for full mouth assessment using 8 periapical radiographs is 23 µSv and the technique is accurate in measuring the root length when the radiograph is taken at 90 º using the paralleling technique; increasing the angle in the bisecting technique will lead to overestimation of the root length (Moze et al., 2013).

2.2.2 Panoramic radiograph

Panoramic radiography is an extraoral radiographic technique that is used to view the entire dentition and their surrounding structure from condyle to condyle in one image (Brezden and Brooks, 1987).

Panoramic radiography is widely used in dentistry for general and specialized diagnostic objectives (Rushton et al., 1999).

Panoramic radiographs were introduced in 1934, and the succeeding years have witnessed continual improvements in both equipment and procedure. The image can be obtained with the subject sitting, prone, or upright. Whichever position is chosen, the patient must remain completely still during the procedure, and the manufacturer's instructions followed meticulously. The image is recorded by the receptor as both it and the beam generator rotate around the subjects head (Rushton et al., 1999).

Techniques for digital panoramic radiography, especially solid-state digital X-rays units (charged coupled device [CCD]-based systems) and photo-stimulateable phosphor plate systems with conventional panoramic units have been developed and have been available commercially for two decades (Farman and Farman, 2000). Several studies found no significant difference between the image quality of digital and conventional panoramic radiographs (Gijbels et al., 2000; Kaeppler et al., 2000; Farman and Farman, 1998). However, no study has been made of whether a possible difference would affect the diagnostic outcome (Syriopoulos et al., 2000).

The jaw is a curved structure resembling the shape of a horseshoe. Panoramic radiography is a two dimensional dental X-ray examination producing a flat image of the curved structure. It is typically set to provide details of the bones and teeth (El-Angbawi et al., 2012).

Most of studies involving panoramic radiographs have evaluated the position of mandibular third molars as well as dental anomalies and bone pathologies. Using panoramic radiographs to assess tooth morphology gives poor diagnostic accuracy about tooth anatomic form and structure (Bell et al., 2003). In addition, it lacks accuracy as a means of screening the anterior maxilla prior to orthodontic treatment (Witched et al., 2010).

Periapical radiography has been shown to be superior to panoramic radiographs in detecting and accurately imaging osseous defects (Pepelassi et al., 2000).

2.2.3 Cone beam computed tomography

Cone beam computed tomography (CBCT) was initially developed for angiography (Robb, 1982), but has been subsequently adapted for use in other medical applications including radiotherapy guidance (Cho et al., 1995) and mammography (Ning and Chen, 2002). This technology made its appearance in dentistry in 1998 in Europe (Mozzo et al., 1998) and approved for use in the USA in 2001 (Hatcher, 2010). The future impact of CBCT on dentistry and more importantly in orthodontics, was firstly addressed by Kapila and Farmand (2003). It has been used to produce 3D digital imaging of anatomic dental and craniofacial morphology by exploiting its ability to produce 3D direct imaging instantly with minimal patient discomfort comprising its primary advantage (Mah et al., 2010).

CBCT Imaging involves an X-ray source and detector mounted on a rotating gantry. A diverging pyramidal or cone-shaped beam of ionizing radiation passes through the center of the area being examined and strikes an area of X-ray detector on the opposite side. Both the X-ray source and the detector pivot around a fulcrum located within the center of the area being examined. During the rotation, which can involve a partial or complete arc, a series, ranging from 150 to in excess of 600 of planar images of the field of view (FOV) are recorded. The difference between this procedure and the more traditional medical CT, is that the latter uses a fan-shaped X-ray beam progressing in a helix to record slices of individual images before stacking them to produce a 3D representation. Each of these slices involves both a separate scan and a separate 2D reconstruction. With CBCT exposure, the entire Field of View is encompassed in one rotation of the gantry during which the sequence produces sufficient data to enable image reconstruction (Scarfe and Farman, 2008).

The technique came into being as a more rapid and convenient alternative to both forms of conventional CT, fan-beam or spiral-scan, and has added advantage or requiring a less costly radiation detector. Among the obvious advantages of this system, in addition to reduced examination time, are a reduction in any image un-sharpness resulting from patient movement, a less distorted image by such movements, and a more efficient use of the x-ray tube. However, with larger fields of view, the image quality suffers from greater noise and less contrast resolution due to the receptor detecting larger amounts of scattered radiation (Scarfe and Farman, 2008). The computers with the capacity to process the complex data, have been developed in the last 30 years, as have suitable X-ray tubes able to sustain to continuous exposures required enable. Together, these have allowed clinical systems to be made small enough and sufficiently cheaply to make the technique feasible in dental surgeries.

The emergence of compact high-quality flat-panel detector arrays, and the falling cost of computers able to process image reconstruction, together with much cheaper X-ray tubes with capacity for continuous exposure and, limited-volume scanning has eliminated the need for very rapid gantry rotation speeds (Scarfe and Farman, 2008).

It has only been since the late 1990s that computers capable of computational complexity and X-ray tubes capable of continuous exposure have enabled clinical systems to be manufactured small and economically enough to be used in dental offices. The factors that have converged to make this possible included the development of compact high-quality flat-panel detector arrays, reduction in the cost of computers capable of image reconstruction, development of inexpensive X-ray tubes capable of continuous exposure and, limited-volume scanning eliminating the need for sub-second gantry rotation speeds (Scarfe and Farman, 2008).

The introduction of dental CBCT has considerably expanded the scope of imaging diagnostics but it has its limitations as a routine procedure in this field. Carious lesions cannot be diagnosed accurately adequately and evaluation of filling and prosthetic restorations is complicated due to scattered X-rays artifact (Weber et al., 2015).

CBCT has become increasingly used in treatment planning and diagnosis of implant dentistry and interventional radiology and as a result many other uses in dentistry especially in the field of oral surgery, endodontics and orthodontics have been identified (Hatcher, 2010).

Despite the increasing adoption of this technology in dentistry, its current role in the field of orthodontics is limited to the diagnosis of unerupted tooth positions, supernumerary teeth, root resorption and similar situations. However, its capability of visualizing root morphology and resorption without the superimpositions and

distortions commonly found in conventional radiographic techniques provides a valuable diagnostic tool for orthodontic treatment planning (Kapila et al., 2011).

The controversy over the radiation dose involved in the use of CBCT and the consequent health risk prevent CBCT from being routinely used for diagnostic purposes (Mah et al., 2010). This limitation in orthodontic practices is exacerbated by the financial and convenience factors associated with CBCT equipment when compared to traditional diagnostic records.

Nevertheless, CBCT has been proved to provide accurate measurements, showing 1-to-1 image-to-reality ratio (Lagravere et al., 2008).

Many studies have been performed to assess the accuracy and reliability of CBCT, mainly in the field of endodontics and for the evaluation of root canal morphology (Qiao et al., 2014; Kamtane and Ghodke, 2016; Assadian et al., 2016; Mokhtari et al., 2016).

In the field of orthodontics the most common and routine form of radiographic imaging are panoramic radiographs. But this imaging is not an accurate means of screening teeth morphology precisely, especially in anterior maxilla locations (Witcher at al., 2010). This has resulted in CBCT being utilized increasingly in the field of orthodontics for diagnosis treatment planning and research, particularly since it incorporates 3D imaging technique which has relative advantages over 2D radiography. Its use in the detection of resorption, supernumerary teeth, TMJ pathology, skeletal deformities and alveolar boundary conditions is beneficial but it has to be justified in terms of relative risks when the information could be obtained using other imaging techniques, even though 3D assessment of craniofacial anatomy, root morphology and angulation, airway morphology and the placement of temporary

anchorage devices is beneficial for treatment planning and treatment outcome (Kapila and Nervina, 2015).

2.2.4 Mathematical models

A mathematical model is a description of a system in terms of mathematical concepts and language (Melsen et al., 1989). The use of conventional metrical approach (CMA) consisting of distances, angles, and ratios as a procedure for characterizing the size and shape of complex irregular forms can be considered appropriate for only the simplest of morphologies. If the form contains even moderate irregularities, something characteristic of most biological organisms, difficulties in description arise. To overcome the shortcoming inherent in CMA, mathematical models come in handy. To construct these mathematical models several different approaches are available; of these being a landmark or homologous-point representation and another outline or boundary representation (Read and Lestrel, 1986).

Homologous-points representation, which includes CMA, is based on a set of homologous points or landmarks used to describe the form. The second approach uses the outline or boundary of the form. In order to be able to accurately describe the size and shape of complex morphological forms a numerical method is required. Obviously there should be a relationship between the analytical model and its measurement system (Lestrel, 1989).

Following this approach, to estimate the area of a tooth root , its shape is approximated to that of a cone. To obtain the best possible approximation, a differentiation in the apical region can be applied to a cone, and the remaing part of the root to a truncated cone.The calculation can then be done to estimate the surface of these two geometrical structures (Figure 1) (Melsen et al., 1989).

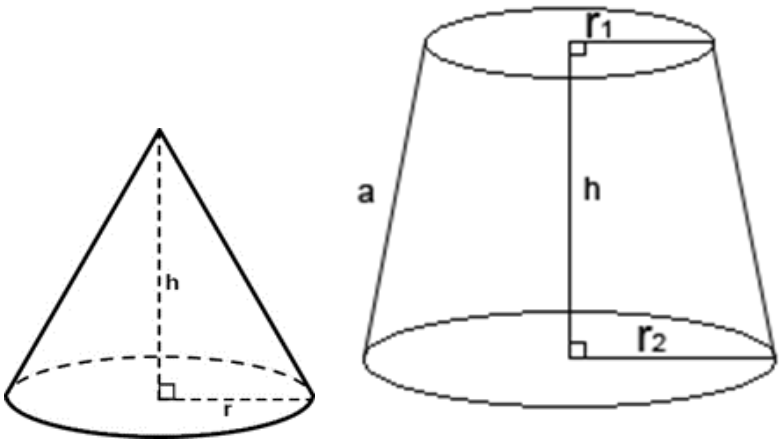

Cone:

h = height

r = radius of base

a = length of side

S = surface area

$S = \pi \, r \, a \; = \; \pi \, r \sqrt{r^2 + h^2}$

Truncated cone:

h = height

r_1 = radius upper base

r_2 = radius lower base

a = length of side

S = surface area

$S = \pi \, (r_1 + r_2) \, a = \pi \; (r_1 + r_2) \sqrt{(r^2 - r^2)^2 + h^2}$

Figure 1. Mathematical model of a cone and a truncated cone used for the calculation of the root surface area. (redrawn from Melsen et al., 1989).

2.3 Digital Models:

Plaster study models have been a reliable and popular forms of making diagnostic records for many years (Stewart, 2001). They provide invaluable information in the field of orthodontics in classifying malocclusions, identifying problems and formulating treatment plans (Peluso et al., 2004). In fact, they can be considered as the primary record used for treatment planning. Studies showed that treatment plans formulated by using study models alone show very little difference from ones using models, photographs, panoramic and cephalometric radiographs and tracing (Han et al., 1991).

Despite their widespread use and acknowledged accuracy as a primary source of diagnostic record, they have many limitations such as breakage, wear and the large volume of storage space they take up (Hurt, 2012).

Digital models alleviate many of the difficulties encountered in using plaster models. They are not subject to physical damage, they require negligible storage space, and they are portable and make excellent tools for patient education. Their use is growing rapidly with trends towards complete digital patient's records for diagnosis, treatment planning and monitoring treatment progress and outcome (Martin et al., 2015). Table 1, which compares plaster and digital models, has been derived from Stewart (2001) but two more variables have been added.

Digital models can be created by two methods, direct and indirect (Nakajima et al., 2007). The direct methods for the creation of virtual models can either be: a direct scan of the dentition with an intraoral scanner using structured light, or using radiographic data such as that from cone-beam computed tomography (CBCT),

magnetic resonance for imaging (MRI), and computed tomography (CT). The virtual dental models derived from CBCT involve radiographic data.

Table 1. Comparison of the features and properties of plaster and digital models [From Stewart (2001) with additional information from the author].

Variables	**Plaster Models**	**Digital Models**
Cost	Less expensive	More expensive
Diagnostic setups	Laboratory procedure	Virtual on computer
Storage space	Large space require	Negligible
Storage cost	Costly	Negligible
Fast and efficient retrieval	Yes	Yes
Retrieval at multiple locations	No	Yes
Subject to physical damage	Yes	No
Transfer of models	Laboratory duplication and shipping	Transfer of digital file
Integration with office management software	No	Yes
Patient education	Yes	Yes
Total space and Bolton analysis	Yes	Yes and faster
Superimposition of treatment outcome	No	Yes

An indirect method, as the name implies, requires additional intermediate steps, such as impression and pouring of the models in plaster, before it can be captured into a digital format. The scanning of an impression or plaster cast can be done by a laser, structured light or even radiographic methods such as OrthoCAD and CAD/CAM. Several errors may occur in this process arising from the choice of process, and the multiple steps employed in scanning and registration.

There are two main requirements to utilize digital models: scanners and digital software.

Scanners produce digital models by digitizing the oral structures directly or indirectly, using intraoral or extraoral scanners. Three types of scanners are used (Persson et al., 2006; Schaefer et al., 2013):

1) Mechanical scanners with touch probe
2) Laser scanners
3) White light scanners

To produce the digital model four types of imaging technologies are employed (Kravitz et al., 2014):

1) Triangulation
2) Parallel confocal
3) Accordion fringe interferometry
4) 3D in motion video

The light, whether laser or white light projected from the light source on the desired object, will reflect back to a sensor or absorbing source. The surface data points are collected to generate a 3D image. As a high-resolution image it must be very accurate in its dimensions, so that the mathematical models and algorithms used to reconstruct

the models provide exact reproduction of the object (Villarrubia, 1997; Axelsson, 1999).

2.3.1 Intraoral scanners (digital impressions):

A 3D intraoral digitizer is used to capture the digital impression. The digitizer uses a camera to capture a video or still image of the target structure. The image is electronically transferred to a facility able to fabricate a model using special software; in doing this, video scans are less accurate than still images (Jeong et al., 2016).

The concept of digital impression and scanning systems was introduced into dentistry in the mid-1980s (Birnbaum et al., 2009). It can avoid errors that are often encountered with conventional impressions such as impression material or plaster model deformation (Ting-Shu and Jian, 2015). Digital scanning offers speed, efficiency, ability to store captured information indefinitely and the electronic transfer of digital images between the dental office and the laboratory (Kim et al., 2013).

Digital impressions have additional advantages such as improved patient acceptance, reducing the distortion of impression materials, 3D visualization, less cost and time effectiveness (Christensen, 2009).

The first digital impression system to be available commercially was introduced by CEREC in 1987. This used a 3D scanner in conjunction with optically active powder on the teeth to create virtual model (Mörmann et al., 1989; Mörmann, 2006). This system was the leader in the field for nearly 20 years. In 2009 BlueCam was introduced; this captures highly detailed images using a powerful blue light-emitting diode.

Nowadays a number of competing technologies entered the market, among which is the E4D™ dentist system. This was introduced in 2008 and was one of the first eliminated the use of a powder in most instances.

Several studies have been performed comparing the accuracy of digital models acquired by direct intraoral scanners with conventional dental models (Nadiu et al., 2009; Grünheid et al., 2014). They appeared to produce reliable and accurate models comparable to those from conventional impressions. Although they eliminate the need of impression materials acquiring the digital image is more time consuming (Aragón et al., 2016).

2.3.2. Extraoral scanners:

Extraoral scanners create a digital model from either an impression or a conventional dental model.

Stereo-photogrammetry:

This is a method of acquiring images using one or more pairs of photographs taken simultaneously (Germec-Carkan et al., 2010) the reproducibility and accuracy of the technique has been stated to be "more than sufficient for clinical needs" and has great accuracy than with direct anthropometrics and 2D photography (Lübbers et al., 2010). Stereo-photogrammetry was developed to overcome the limitations of CBCT or laser scanning regarding cost, being invasive (Littlefield et al., 2004) and motion artifacts during long scanning times (Hajeer et al., 2004).

The photogrammetry device takes a set number of pictures per second between two scan bodies and identifies the spatial position of each structure without physical contact. 3D data for each structure are registered in vector format together with their angle, the information is then stored in an STL file (Agustin-Panadero et al., 2015). 3D images are acquired by combining photographs captured from various angles with the synchronous digital camera.

The advantages of this method are lack of motion defects because of short imaging time, high color resolution, quick configuration and imaging via advanced software (Brons et al., 2012; Kochel et al., 2010).

Laser or white light scanners:

Almost all dental 3D scanners use a similar fundamental principle. Basically the 3D scanner comprises one or several cameras, a source of light and a multi-axial motion system for locating the object to be scanned in the right position relative to the cameras and light source. The light source illuminates the object with well-defined lines which the camera records as images. Since the angle and distance between light source and camera are known, trigonometry can be used to calculate the points from which the light is reflected. Although this process of "triangulation" can be performed with a single camera, multiple cameras improve speed, coverage and accuracy. The lines of projected light are used to produce 3D contour lines. The relative motion between the scan head comprised of the camera and light source and the object result in multiple lines, which convert into multiple 3D contours. Laser scanners produce a series of lines when the scan head moves along a precise linear axis. White light scanners employ a fixed scan head, but consecutively project a series of shifting line patterns from one central position. Thus the two variations of the technique are based on the same principle. This makes it difficult to claim that either is better than the other in terms of their scientific principles (Hollenbeck et al., 2012). Some authors may disputet this statement on the grounds that the scanning, in particular, the scanning of highly reflective surfaces (e.g., metal) using lasers can potentially influence outcomes.

CBCT-derived digital models:

CBCT imaging can take 3D images using the most up-to-date scanning techniques that involve minimal patient discomfort. They can provide instant results, although their

radiation dose is higher than conventional radiographic techniques, but still significantly lower than multi-slice CT (Silva et al., 2008). CBCT can develop a digital model from the radiographically scanned dentition and relevant studies claimed that the digital models produced using CBCT are as accurate as OrthoCad digital models in terms of accurate linear measurements (Kau et al., 2010). According to the relevant statement, these models are not only highly accurate, but easily reproducible (Maroua et al., 2016). However, objections might be raised concerning the considerably lower levels of resolution obtained in the digital models obtained from CBCT images compared with white-light scanning of models because the voxels size is relatively large.

More recently, direct scanning of alginate impressions using cone-beam computed tomography (CBCT) has been introduced to eliminate the need for plaster pouring. However, when the impressions are not stored under special conditions, they should be scanned immediately, or at least within 2 to 3 hours after they are taken to produce accurate and reliable result (Jiang et al., 2016).

Since the introduction and incorporation of digital models into the field of dentistry, especially orthodontics, many studies have been performed to evaluate their accuracy and reproducibility. These models can provide diagnostic information similar to caliper measurements (Akylacin et al., 2013). They can be used to provide very accurate measurements of tooth dimensions (Horton et al., 2010). Study model analysis routinely used in orthodontics, such as Bolton analysis are faster than, and as accurate as, the traditional methods and clinician can use the method confidently for diagnostic purposes (Mullen et al., 2007).

2.4 Root morphology assessment from digital models

By using the Ortho Insight 3D ™ high-resolution laser scanner on either models or impressions in conjunction with Motion View Software, LLC (Chattanooga, Tennessee., USA) different analyses on dental arches can be made. These include measurements of dental arch dimensions, space analysis and tooth size discrepancies (Bolton analysis). After the scanning of models or impressions, the electronically produced images do not only include the crowns of the teeth but also indicate their roots with the use of specific mathematical/geometric predictions. To the best of our knowledge, the existing bibliography does not contain any study that has evaluated the accuracy of this prediction. On the other hand, many studies have evaluated the accuracy of CBCT images with reference to different teeth locations (Flores-Mir et al., 2014; Yang et al., 2013; Benninger et al., 2012).

Hence, the assessment of the accuracy of root morphology prediction derived from digital models elaborated by the Ortho Insight 3D ™ software can be tested by comparison with root morphology images derived from CBCT registrations.

SPECIAL PART

3. Research Hypotheses

Hypothesis to be tested is set as:

There are differences in predicted root inclination characteristics generated by commercially available 3D laser scanner software and the inclination characteristics derived from CBCT data.

Null hypothesis:

There are no differences in predicted root inclination characteristics generated by commercially available 3D laser scanner software and the inclination characteristics derived from CBCT data.

.

4. Aim

The aim of this study was to assess the accuracy of digital models generated by a commercially available software in predicting anterior teeth root inclination characteristics by comparison to relevant data obtained from CBCT images.

5. Material and Methods

5.1 Subjects

In this retrospective study pre-treatment maxillary and mandibular plaster models and the corresponding CBCT scans of 31 consecutive patients attending a private orthodontic clinic in Beirut, Lebanon, who fulfilled the following inclusion/exclusion criteria, were selected. All subjects were medically fit and healthy, in permanent dentition, with normal tooth crown morphology. Patients who had extensive anterior edentulous regions (more than one tooth missing), with abnormal tooth morphology, history of tooth trauma, history of previous orthodontic treatment, presence of restoration that altered the mesio-distal width of the crown, congenitally missing teeth, history of interproximal reduction and craniofacial anomalies or syndromes were excluded. The selected patients represented both genders (males: 10; females: 21), ranging in age from 12 to 40 years (mean: 19.2 years; S.D.: 8.12 years). Patients were characterized by different malocclusions (Class I; Class II, division 1; Class II, division 2; Class III).

5.2 Materials

Each plaster model was scanned with the Ortho Insight 3D ™ scanner (Motion View Software, Chattanooga, Tennessee, USA) with the resolution set at ‘‘high’’ using the supplied software (version 6.0.7044).

CBCT scans were taken using a Kodak 9500 Cone Beam 3D System (Carestream Health, Inc., Rochester, New York, USA) according to the following settings: 206 mm x 184 mm large field of view, 0.3 mm slice thickness, 60 – 90 kv tube voltage pulsed mode, 2–15 mA tube electric power, 140 kHz frequency, focal point at 0.7 mm, 2 mn

and 20 sec. reconstruction time. The images obtained were converted to DICOM (Digital Imaging and Communications in Medicine) format and analyzed using the Viewbox software, version 4.1.0.1 BETA (dHAL, Kifissia, Greece).

Based on the information provided to the author of this investigation, CBCT scans had been obtained at the private orthodontic clinic only when there had been appropriate reasons indicating their utility over alternatives (Isaacson et al., 2015).

This research was approved by the Research and Ethics Committee of Hamdan Bin Mohammed College of Dental Medicine, Mohammed Bin Rashid University of Medicine and Health Sciences (Ref: EC0315-004).

5.3 Methods

Evaluation of plaster models and CBCT data included only anterior teeth because a preliminary visual evaluation of digital models showed gross errors in the root imaging of posterior teeth, thus suggesting their exclusion from this study. In addition, anterior teeth are simpler in terms of morphology of both their crowns and roots.

Elaboration of data took place according to the following steps:

- Each patient's maxillary and mandibular plaster models were scanned using the Ortho Insight 3D ™ laser scanner (Figure 2).
- Upper and lower models were aligned (Figure 3). Digitizing the models started by separating the teeth (Figure 4).
- Landmarks were detected and were set by the author in order for the software to recognize the tooth and perform analysis (Figure 5). They included a total number of 8 points for incisors and 3 points for canines (Table 2).
- Facial axes were detected and were set by the author (Figure 6).
- Care was taken that alignment of roots with crowns should not change (Figure 7) and models were exported to a STL (Stereo lithography) file format which is readable by the Viewbox software (Figures 8).
- Models with STL file format were loaded in Viewbox software (Figure 9), unnecessary parts were removed (Figure 10) and a new mesh containing only the crowns of teeth was created (Figure 11). CBCT images were loaded in Viewbox using DICOM file format (Figure 12) and a mesh with only crowns of teeth was created (Figure 13).
- The CBCT and digital models meshes were aligned in two stages: an initial manual alignment followed by a precise adjustment performed automatically

using the Iterative Closest Point algorithm (ICP) (Besl and McKay, 1992) (Figure 14).

- To determine the line resembling the long axis of the root of a tooth on digital models, the best fit line to 50 points lying on the root surface was computed without using apex points in computation due to their large variation (Figure 15).
- To compute the long axis of a root in CBCT, a slice object, oriented perpendicular to the long axis of the tooth that shows cross sectional slices of the tooth was created (Figure 16).
- A path for slices was created from cervix of the tooth until root apex (Figure 17).
- At predefined positions (0%, 20%, 40%, 60%, and 80%) along the long axis a root boundaries were drawn (Figure 18).
- The points were automatically placed at equidistant positions along the curves and the line resembling the long axis was computed (Figure 19).
- The final result showed the angle between two axes: namely the one derived from digital models, and the one from the CBCT images (Figure 20).

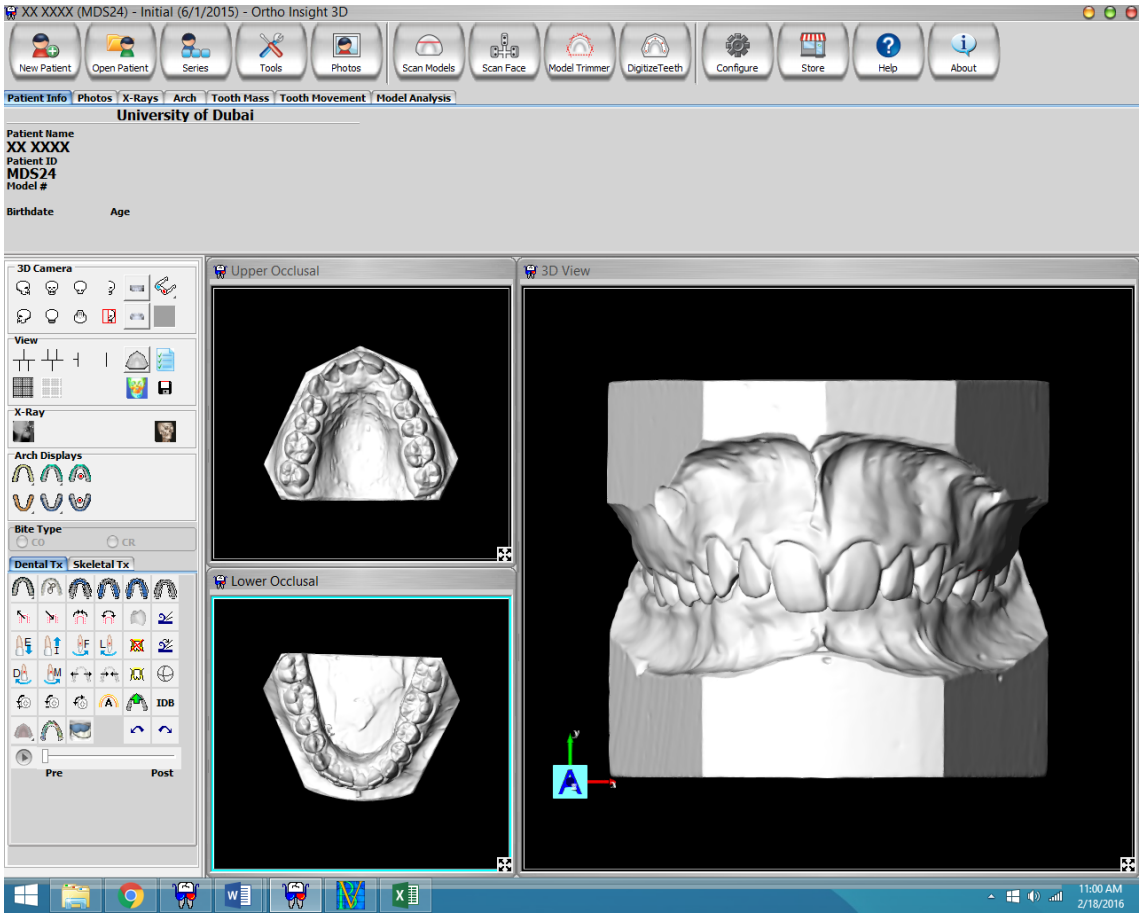

Figure 2. Scanned model in Ortho Insight 3D scanner software. (Courtesy of Motion View Software LLC; printed with permission)

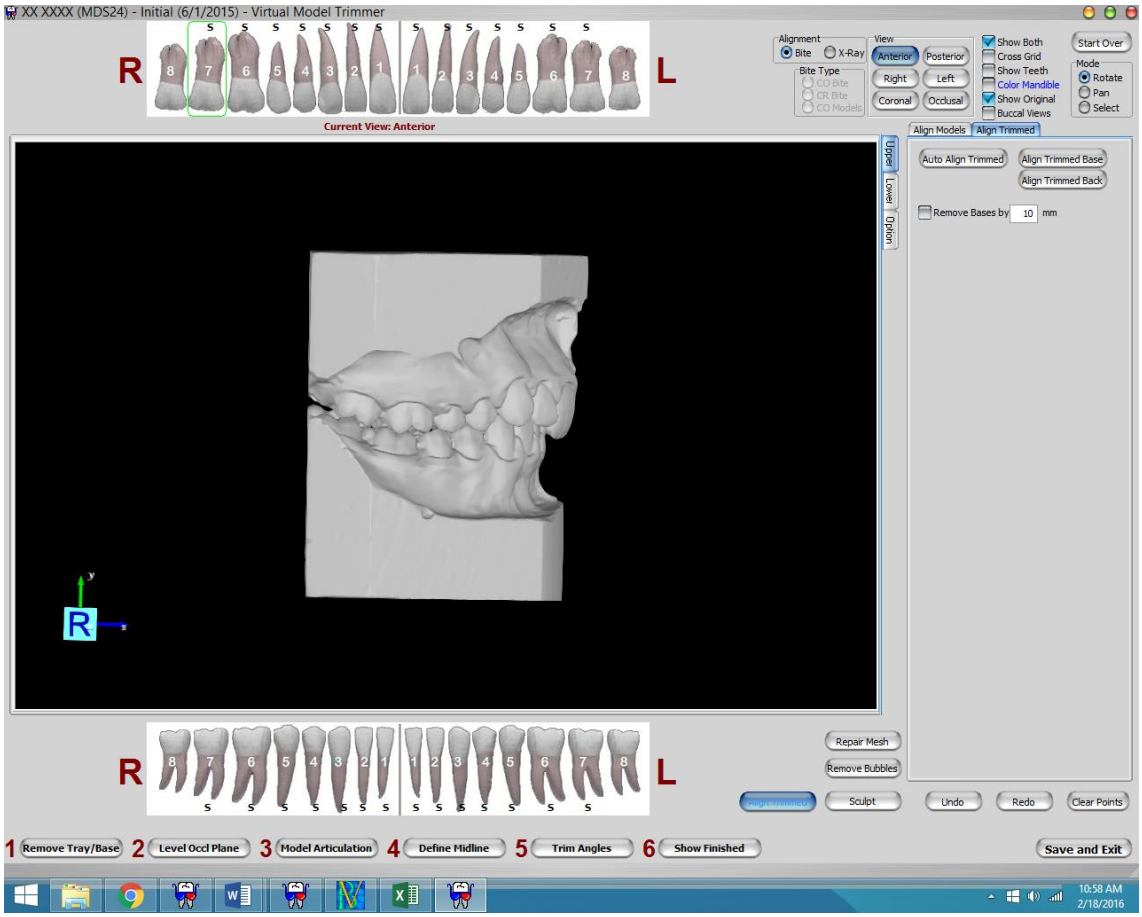

Figure 3. Aligned upper and lower models. (Courtesy of Motion View Software LLC; printed with permission)

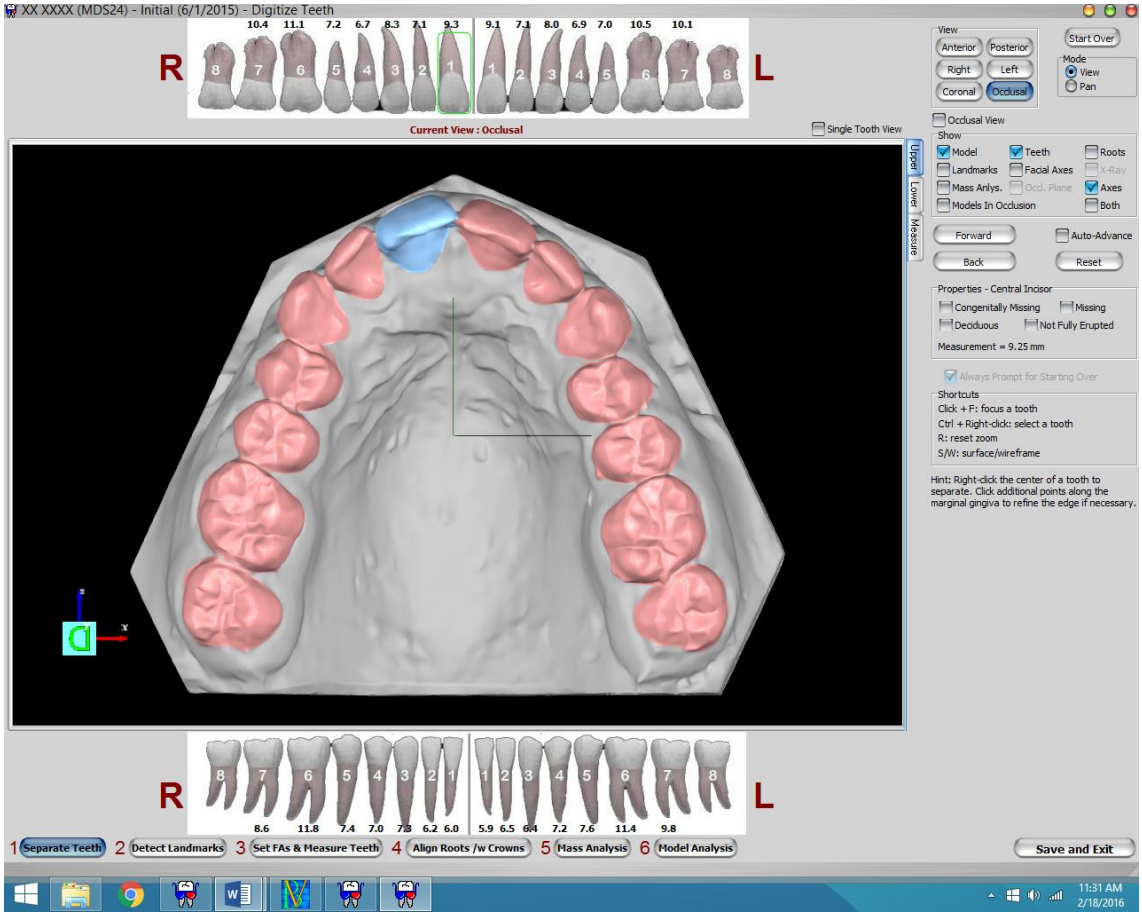

Figure 4. Initiation of digitizing by separating teeth. (Courtesy of Motion View Software LLC; printed with permission)

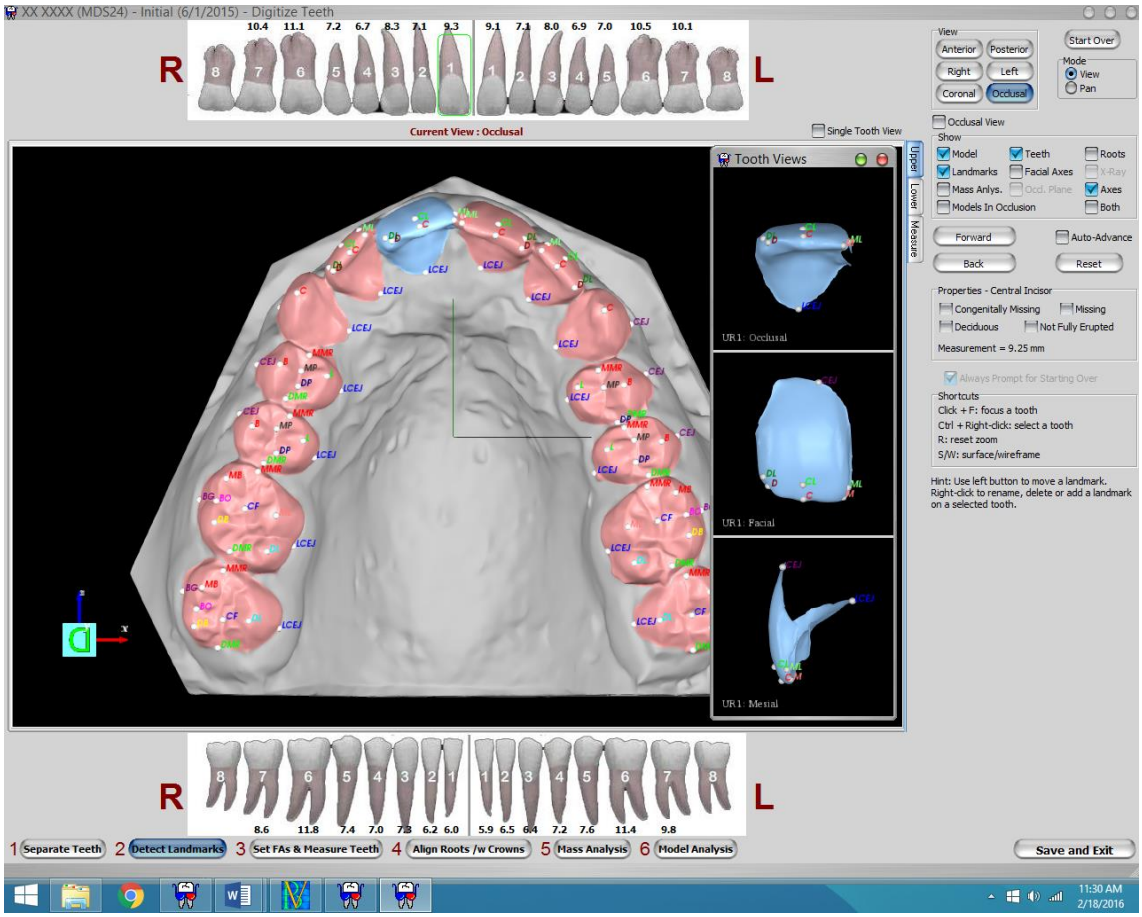

Figure 5. Landmarks detection. (Courtesy of Motion View Software LLC; printed with permission)

Table 2. Landmarks of teeth to be detected by operator on Motion View software.

Landmarks	**Teeth**
Central-Labial	Maxillary and mandibular central and lateral incisors
Central-Incisal	Maxillary and mandibular central and lateral incisors
Mesio-Labial	Maxillary and mandibular central and lateral incisors
Mesio-Incisal	Maxillary and mandibular central and lateral incisors
Disto-Labial	Maxillary and mandibular central and lateral incisors
Disto-Incisal	Maxillary and mandibular central and lateral incisors
CEJ Facial	Maxillary and mandibular central and lateral incisors and canines
CEJ Lingual	Maxillary and mandibular central and lateral incisors
Cusp	Maxillary and mandibular canines

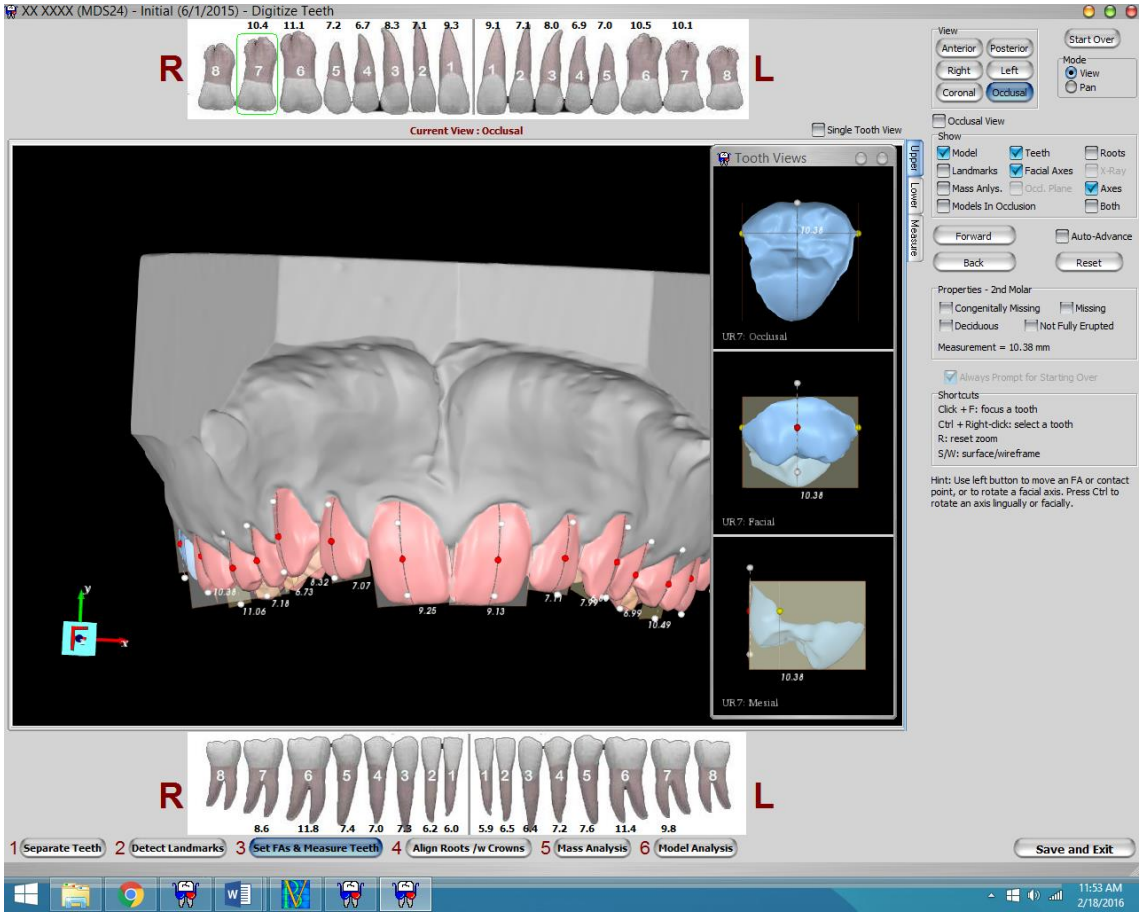

Figure 6. Setting of facial axis. (Courtesy of Motion View Software LLC; printed with permission)

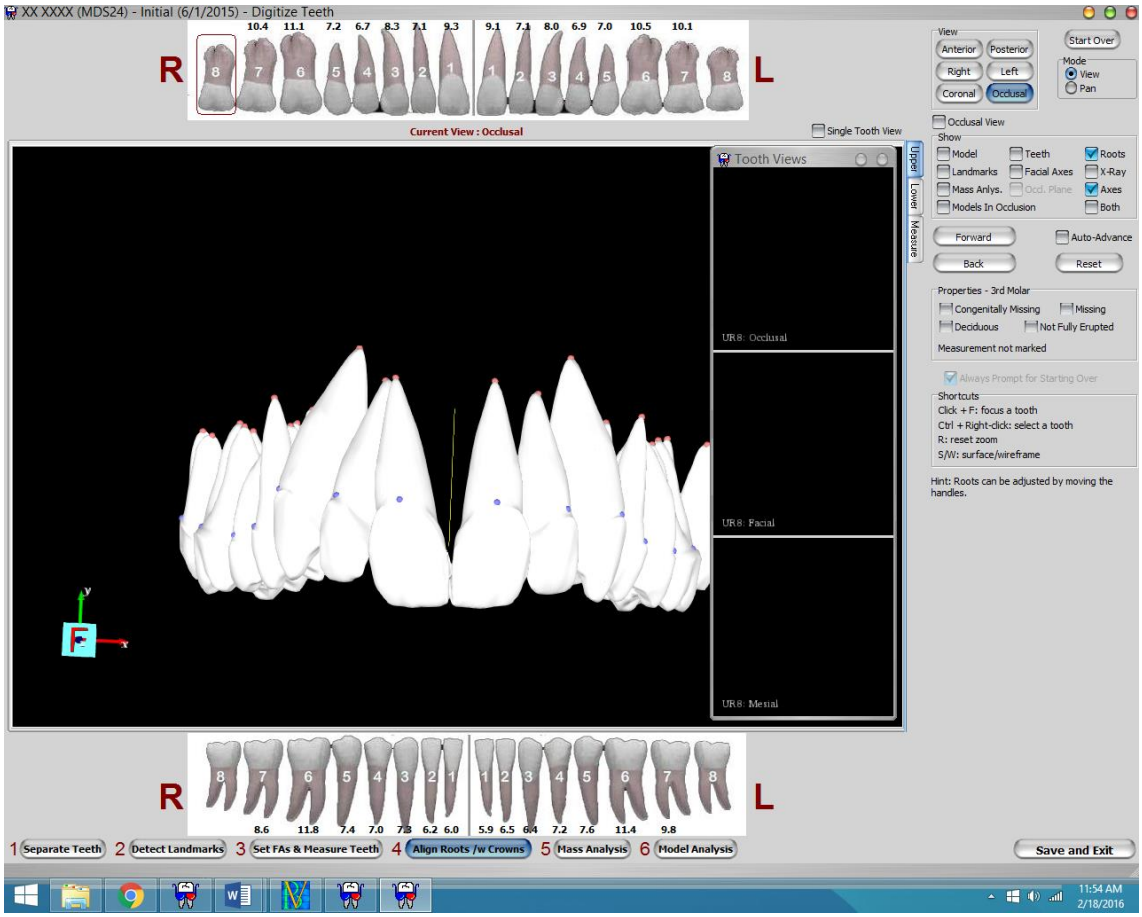

Figure 7. Untouched root and crown alignment. (Courtesy of Motion View Software LLC; printed with permission)

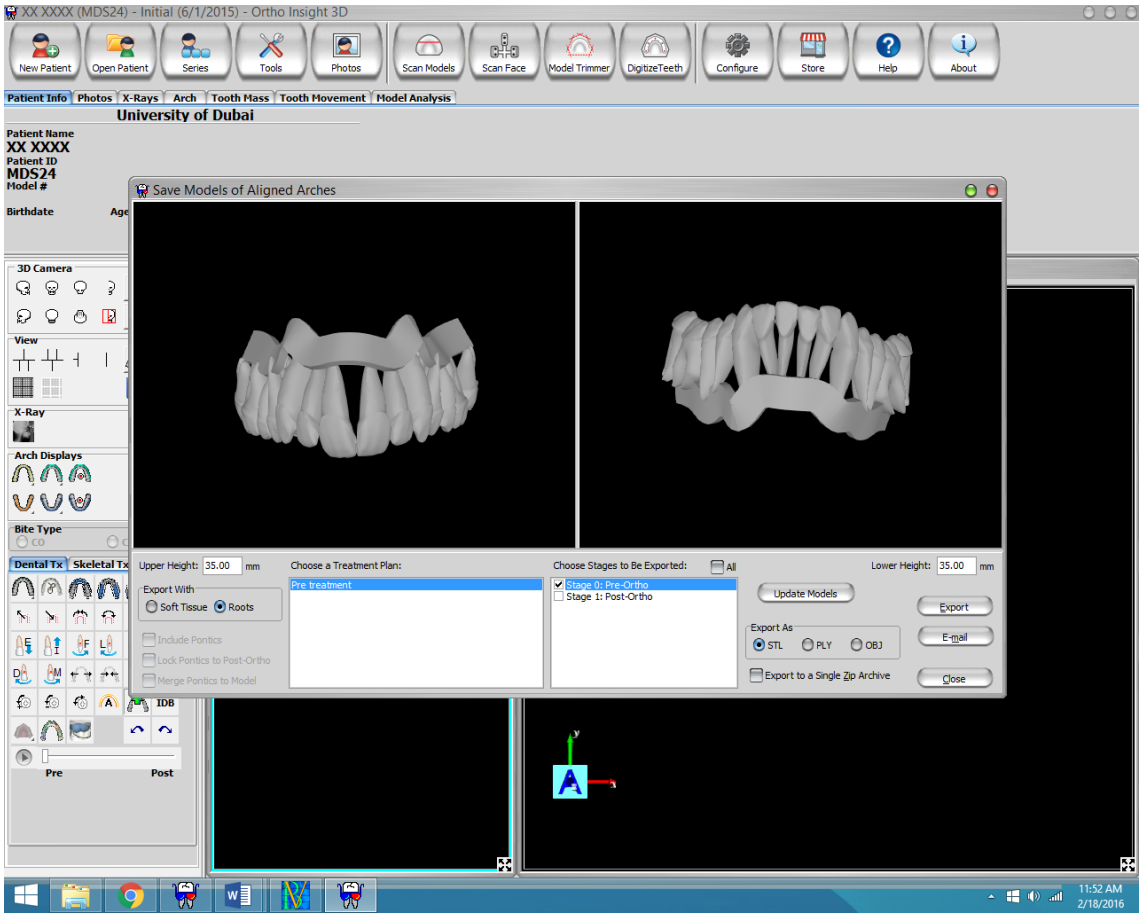

Figure 8. Exporting of digital models to STL file. (Courtesy of Motion View Software LLC; printed with permission)

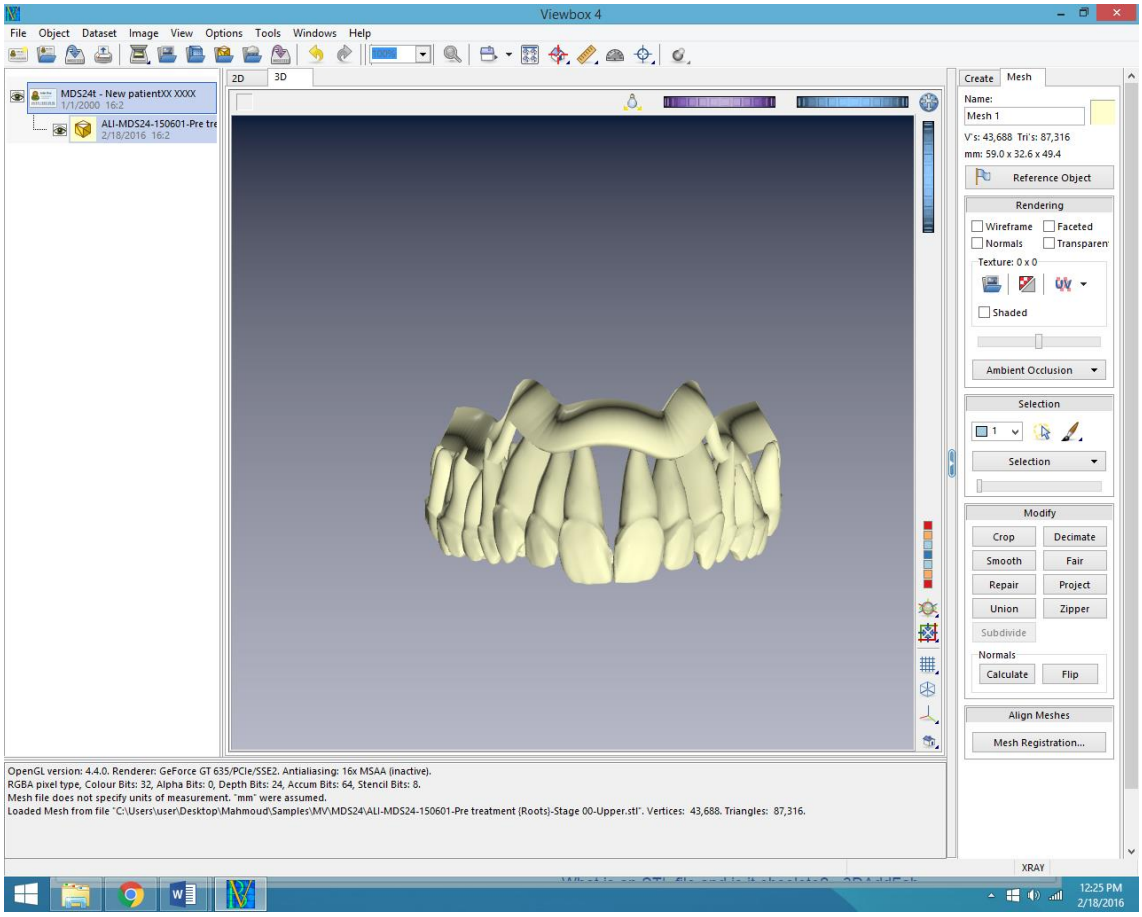

Figure 9. Uploading of digital model to Viewbox software.

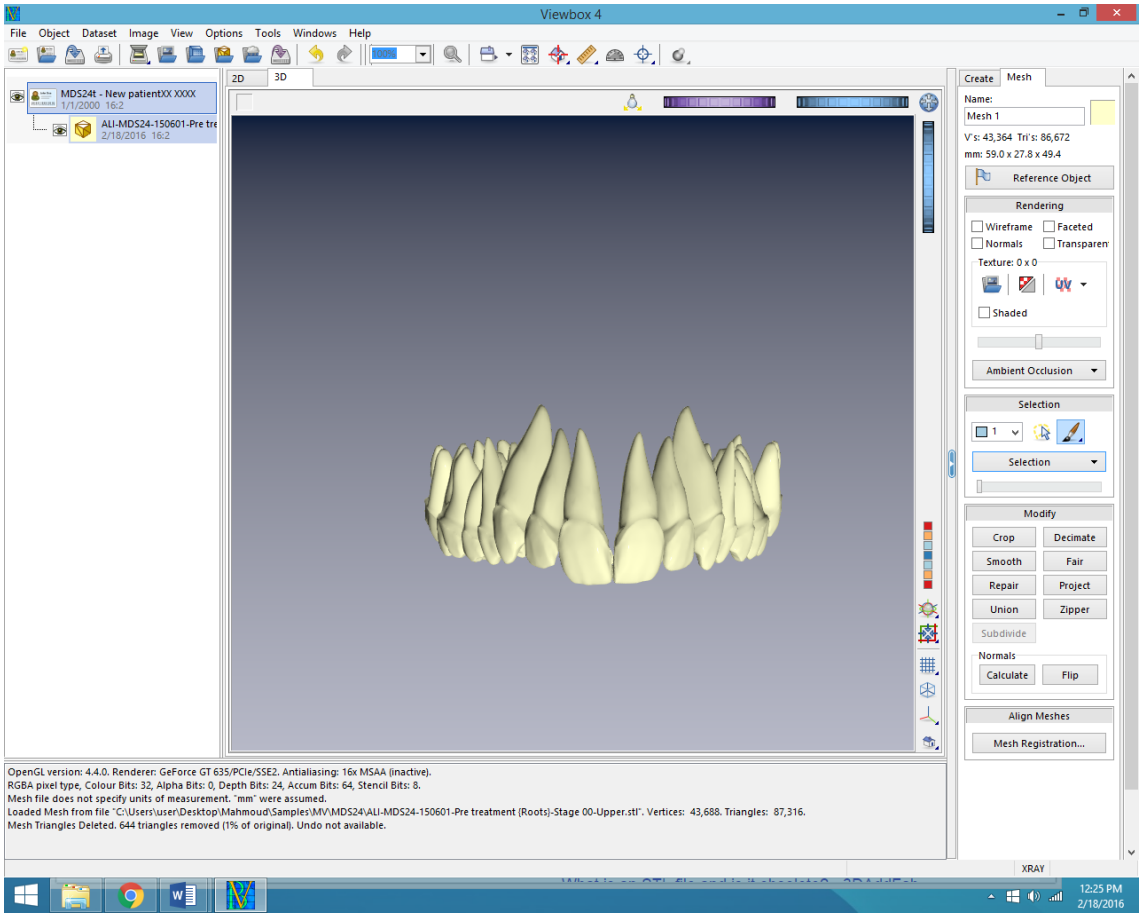

Figure 10. Deleting unnecessary parts.

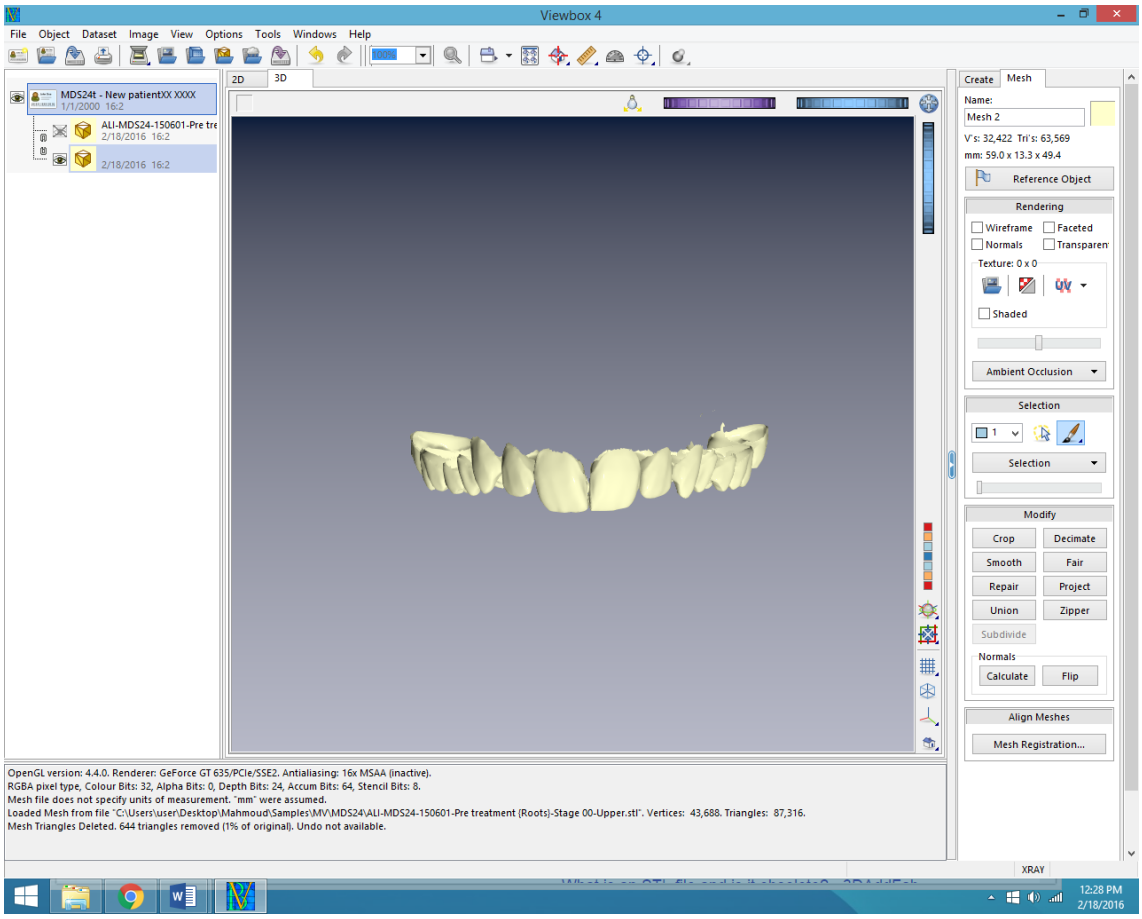

Figure 11. Creating a new mesh consisting of crowns derived from digital model.

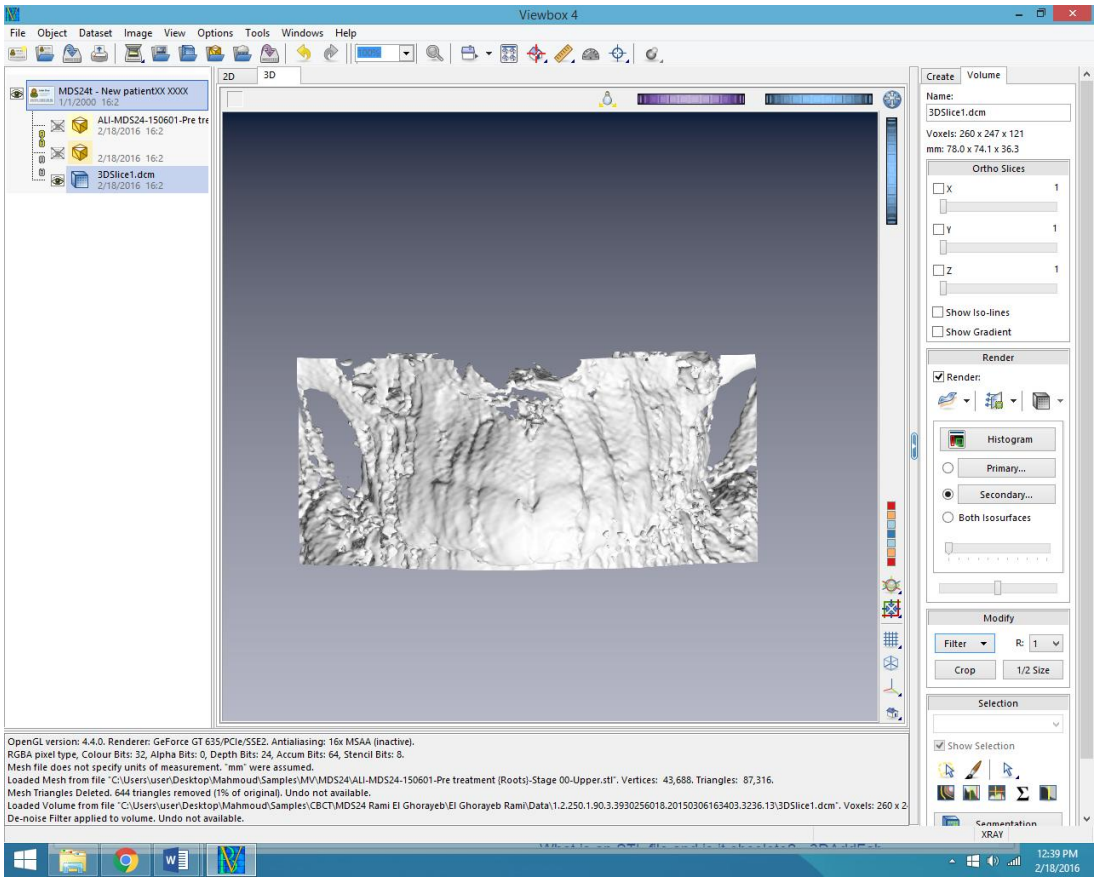

Figure 12. Uploading CBCT images to Viewbox software.

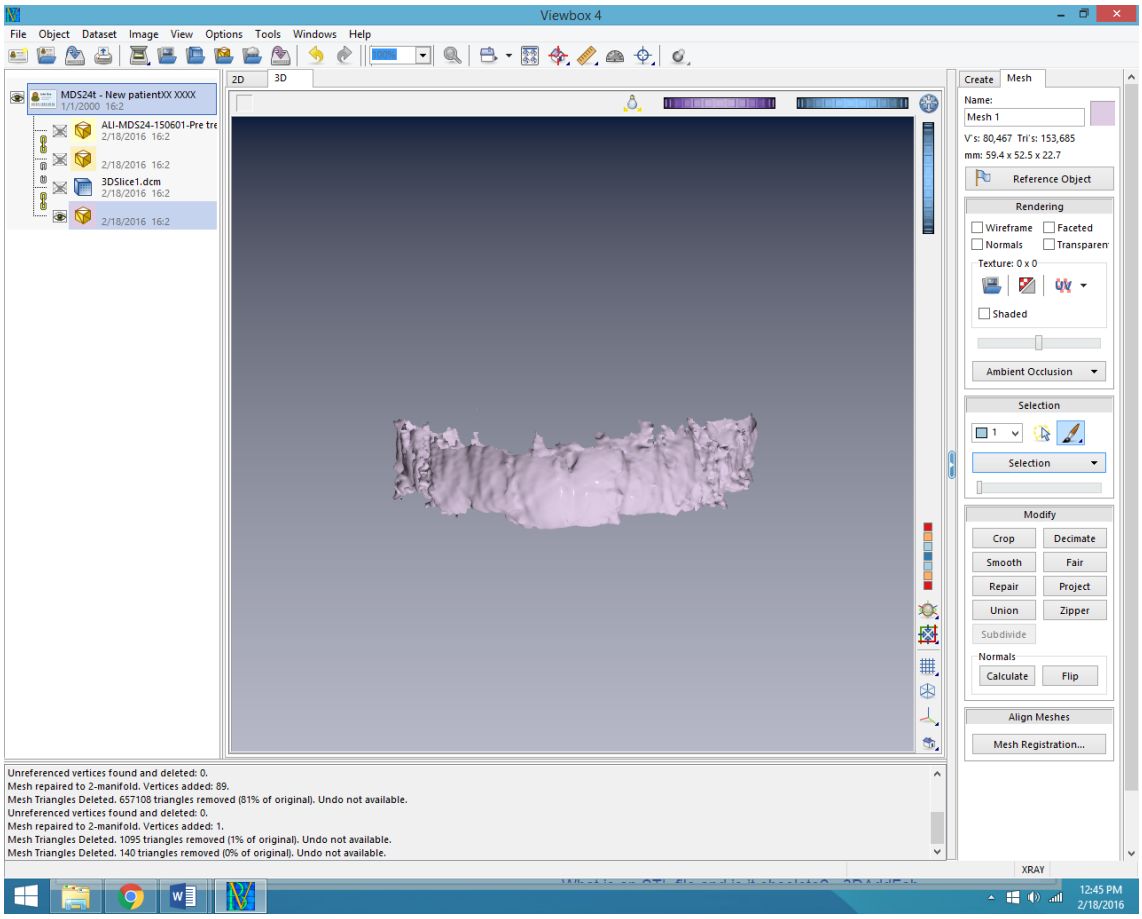

Figure 13. Creating a new mesh consisting of crown derived from CBCT.

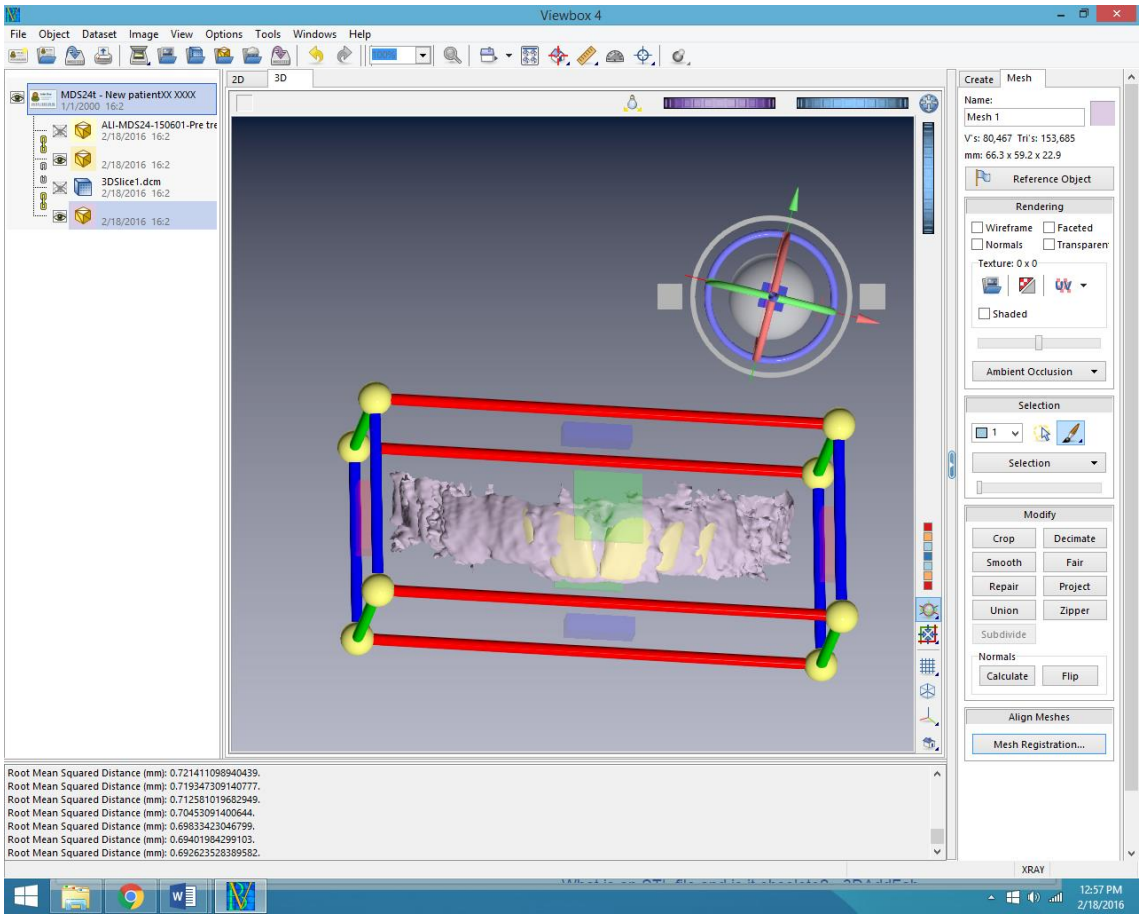

Figure 14. Alignment of CBCT and digital model meshes.

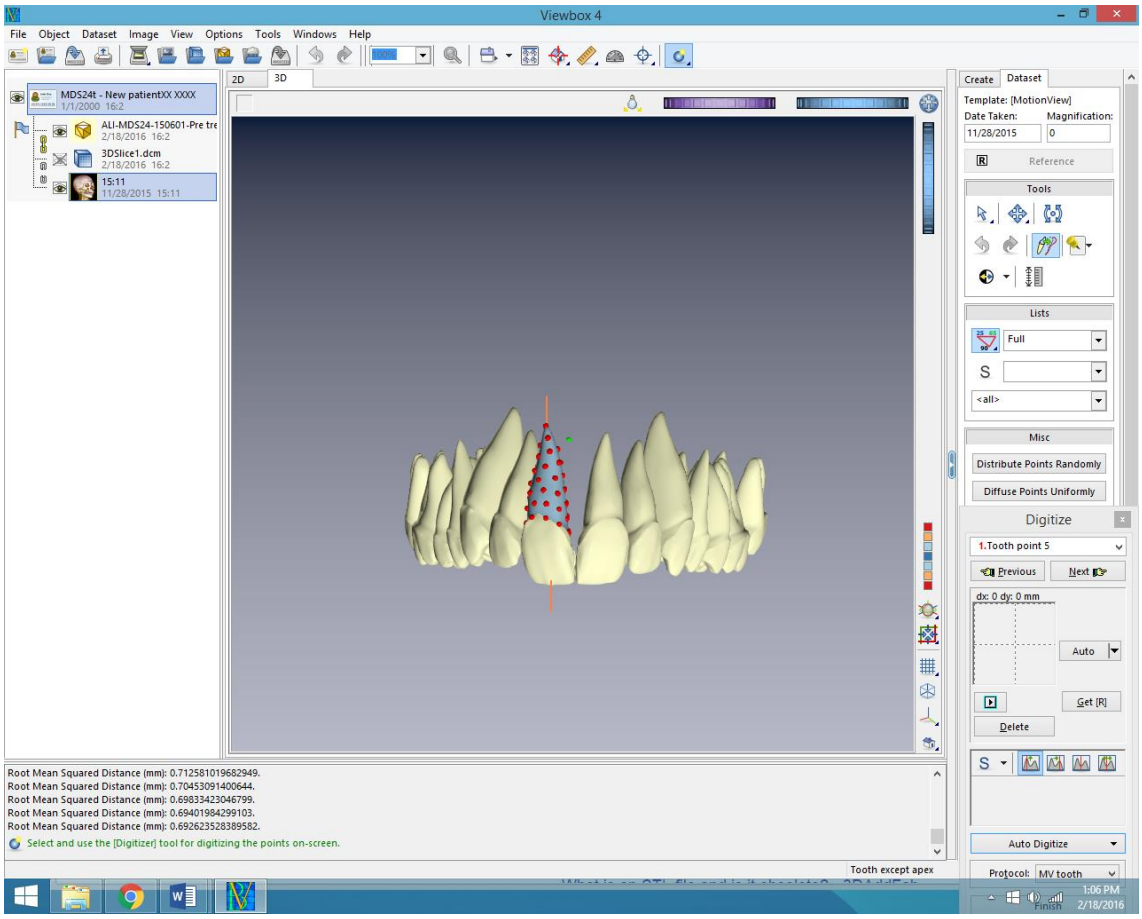

Figure 15. Surface computation of digital model's root to determine its long axis.

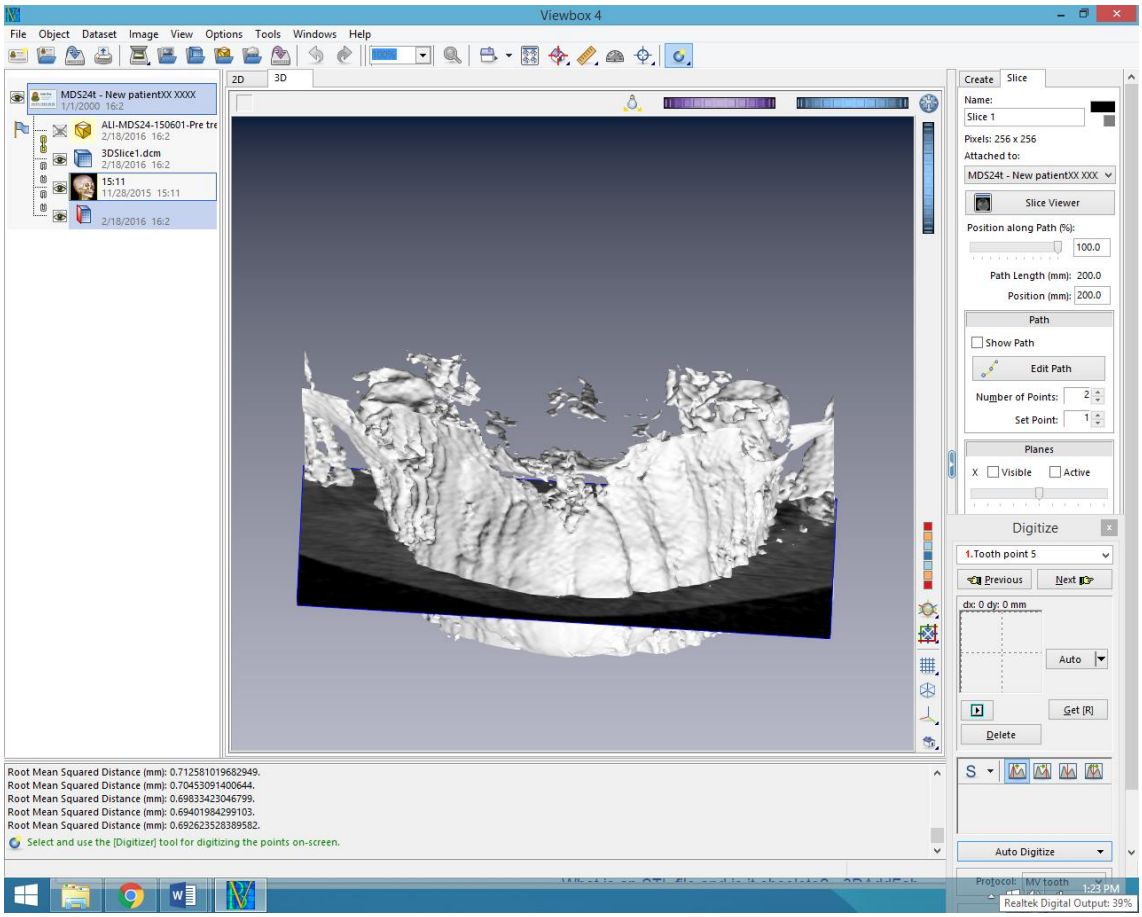

Figure 16. Creating a slice perpendicular to long axis of root in CBCT.

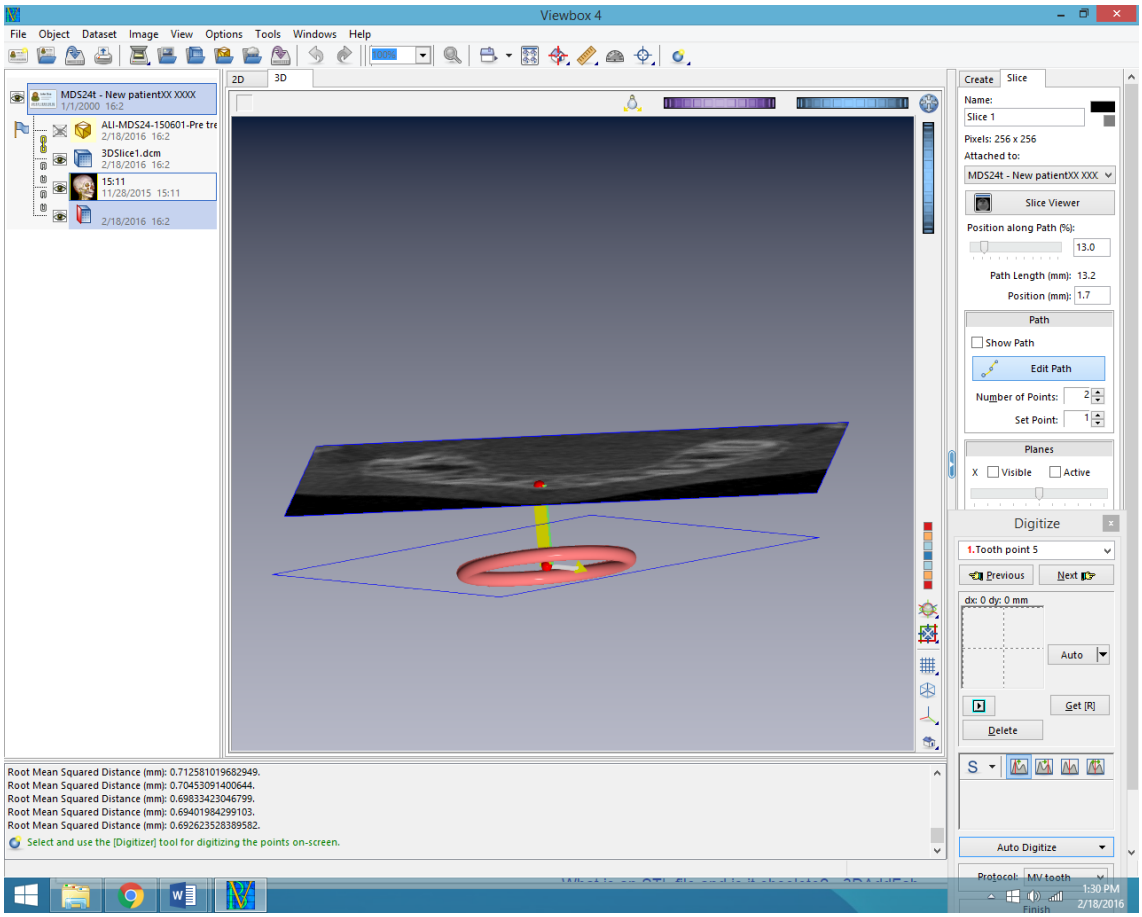

Figure 17. Creating a path from cervix to root apex in CBCT.

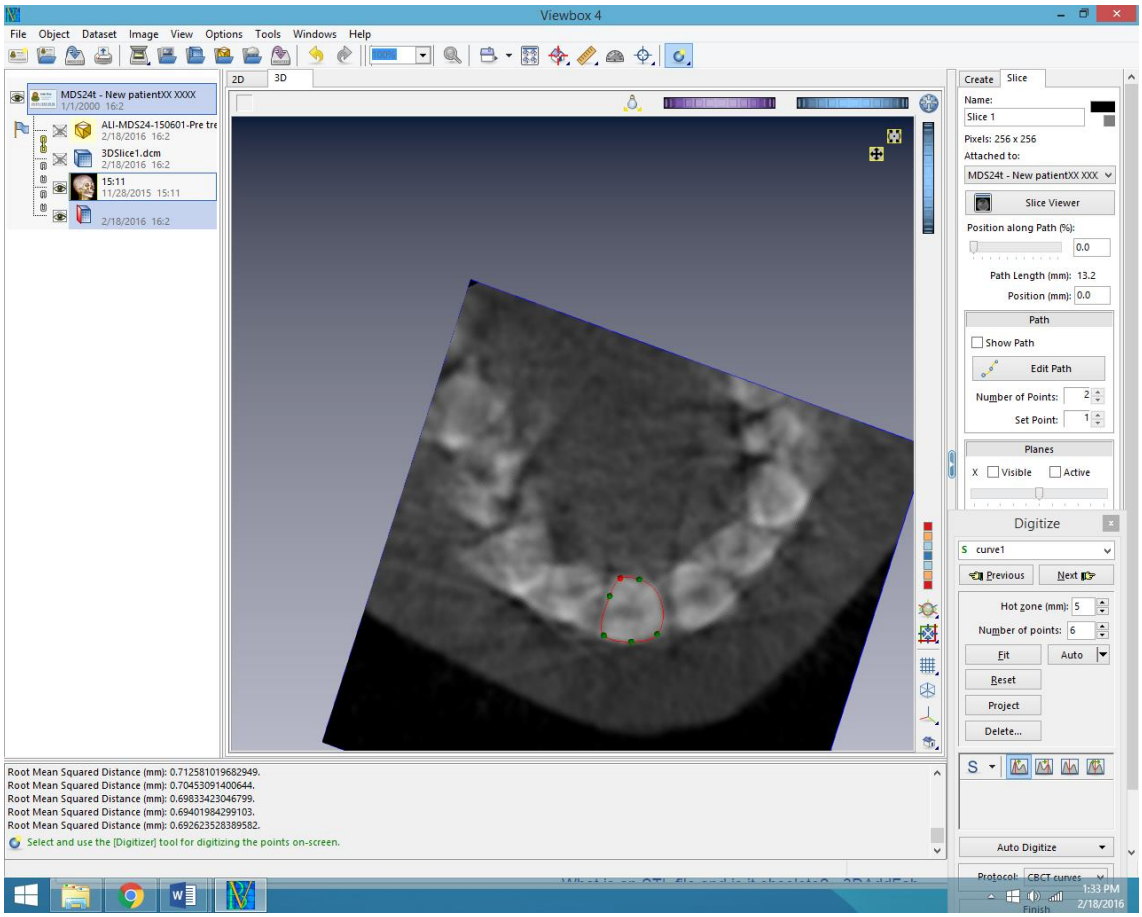

Figure 18. Detecting root boundaries in different cross sections.

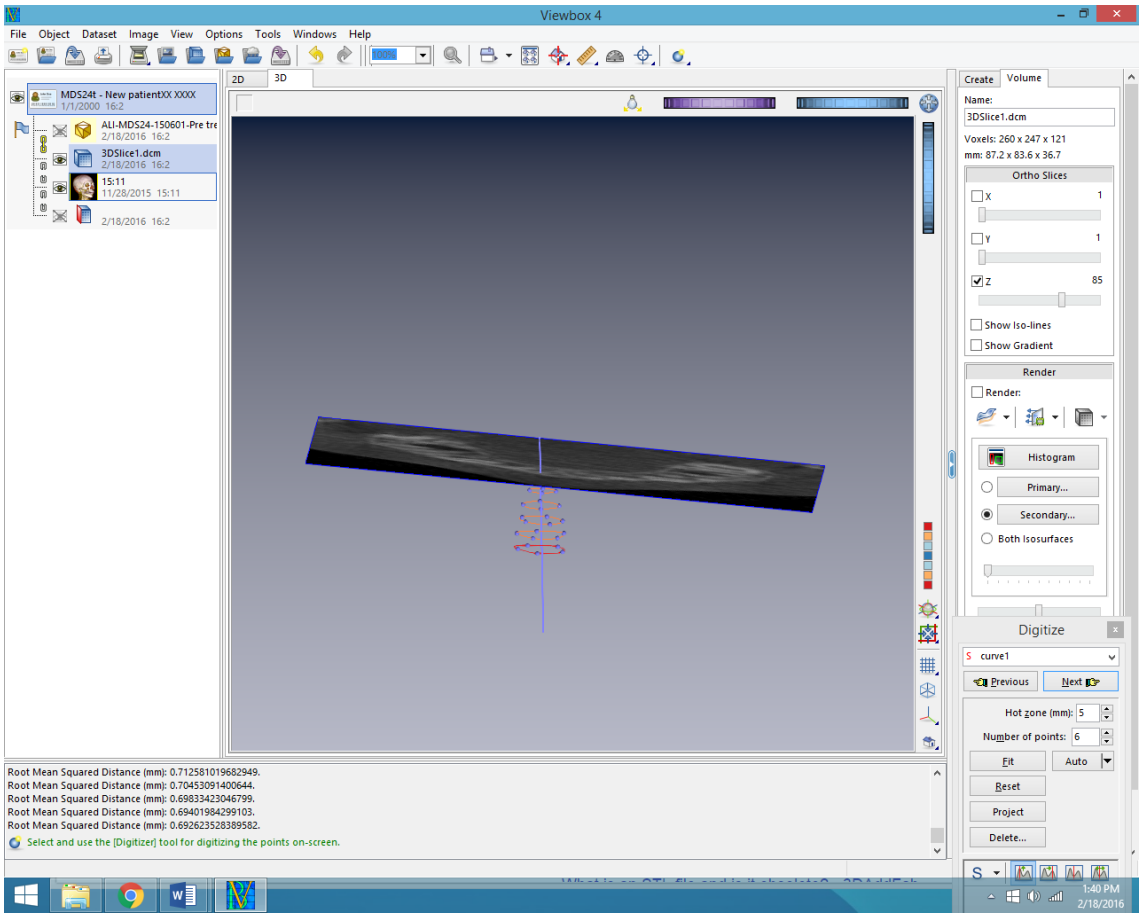

Figure 19. Automatic computation of root long axis in CBCT.

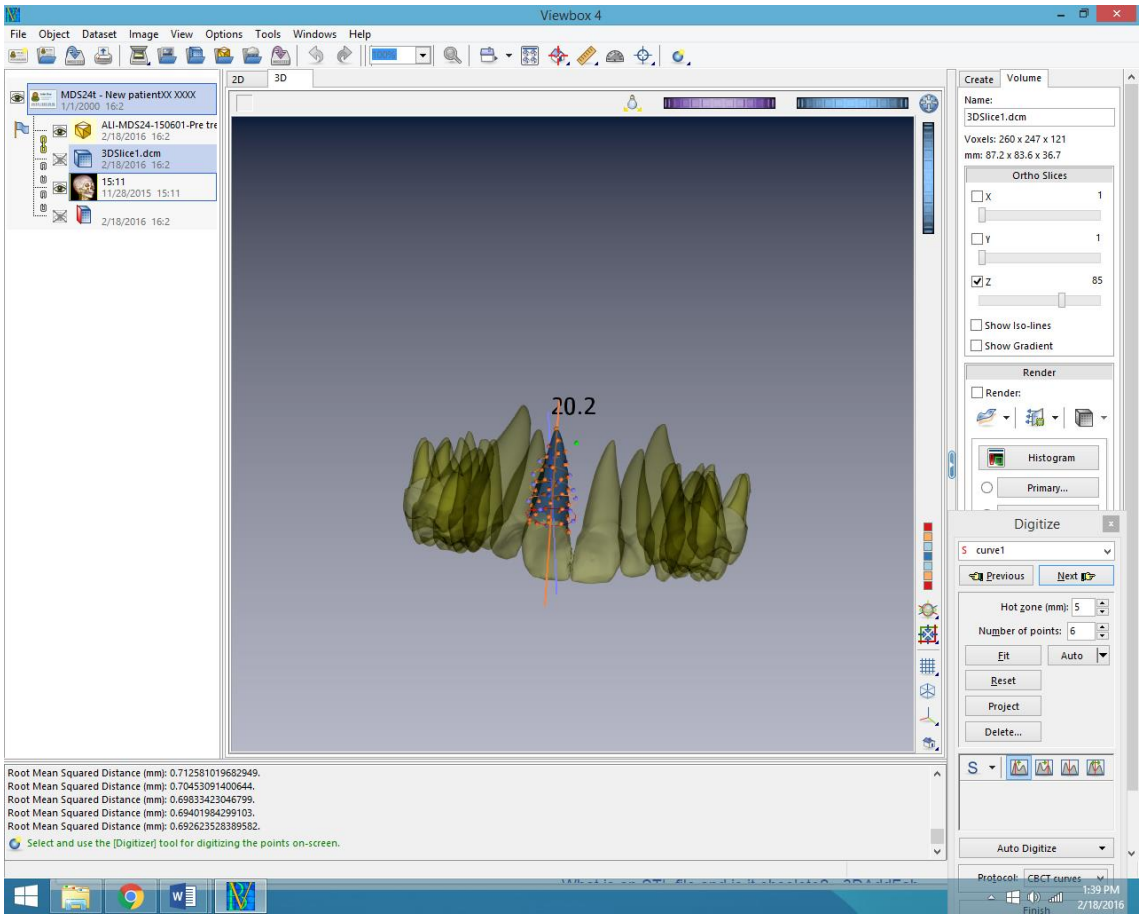

Figure 20. Final result that shows the difference between the two long axes.

6. Statistics

6.1 Sample size calculation

The sample size was calculated using the Cochrane analysis formula that provides sample size and power analysis for hypothesis tests, confidence interval and equivalence analyses. A total sample size of 30 subjects would give a power of 80% with 95% significant level.

$$\Phi(x) = \left[-Z_{1-\propto} + \frac{\Delta\sqrt{n}}{\delta}\right] = 1 - \beta$$

Under the assumption of a unilateral test from the pilot and the literature, the value of $\Delta(\text{difference in average})$ and $\delta(the\ \text{standard deviation})$ will be observed and we fixed our sample size at 30, with the calculation being made accordingly.

6.2 Statistical methods

Data were entered in an Excel file and SPSS for Windows (version 20.0, SPSS Inc., Chicago, Illinois, USA) was used for the statistical tests. Measurements per tooth were tested for normality by using the Shapiro-Wilk test which is valid for small sample sizes. Cross-tabulation was used to examine the independency between categorical variables and statistical analysis was performed using the χ^2 test of association. Where two or more continuous independent variables were examined, the t-test and analysis of variance (ANOVA) were used as adequate if the measurement were normally distributed. In cases of non-normality of measurement, the Mann-Whitney and Kruskal-Wallis tests for multi-comparison of continuous data were used. The paired t-test was used to test the reliability and consistency of the investigator. Where it was thought appropriate, the Neyman-Pearson test was used to examine the linear

correlation between two continuous variables. A P-value of less than 0.05 was considered significant in all statistical analyses.

6.3 Method Error

In order to determine the degree of intra-examiner error of the measurements taken from the two different type of records (digital models and CBCT), 5 patients' records were randomly selected, and all measurements were repeated twice by the author at an interval of two weeks. Then the correlations were computed using the intra-class correlation coefficient (ICC).

The Bland-Altman technique is not available as a procedure in SPSS. However, the method was programmed as follows:

The difference between two dependent measures was calculated between these measures to get the deviation and this newly created value was used to test its average from zero by using one-sample t-test. Then on the second step a new variable was created as an average of each pair of readings and Bland Altman test used the confident limits of the difference to see how the data was distributed between two halves of the plot. In addition, to have real sense of agreement a linear regression was conducted to test the significance of the coefficient of the regression and this is the intra-class correlation coefficient (ICC).

7. Results

On the assumption that parametric tests are more powerful than their equivalent non-parametric counterparts, and can detect differences with smaller sample sizes, or detect smaller differences with the same sample size, a test of normality was performed. The aim was to test normality of measurements of difference between long axes of the root by two methods in each tooth (MDBLAR). The Shapiro-Wilk test was chosen and the results are shown in Table 3. The upper right central incisors, upper right canines, upper left central incisors and upper left canines were not normally distributed (P-values were 0.036, 0.032, 0.013 and 0.013, respectively). However, more teeth (highlighted) demonstrated a probable non-normality distribution.

It was expected that the data would have a non-normal distribution since negative values are not possible, and the ideal angular estimation error would be zero degrees.

To test the assumption that the investigator had read the materials consistently, a test was performed by using paired t-test after blindness and random selection were considered. As shown from the p-value in the last column of Table 4, the reliability of the investigator was confirmed, all the p-values were above 0.05.

The paired t-test was used to analyze the mean differences between the MDBLAR measurements. The intra-class correlation coefficient was used to determine the agreement between the measurements. The p-value was set at <0.05.

Table 5 presents the descriptive statistics data. The maximum angle between the images derived from digital models and CBCT data was almost 40 degrees (upper left canine). The upper right canine also reached the same level of difference. The canines produced the worst results, followed by the lower lateral incisors. The upper central

incisors exhibited the best results, although the maximum angle exceeded 20 degrees (but the median was only around 8 degrees).

Table 3. Test of normality by using Shapiro-Wilk test. P-values that show probable non-normality are highlighted.

Tooth	W	P-value
11 (upper right central incisor)	0.927	0.036
12 (upper right lateral incisor)	0.938	0.073
13 (upper right canine)	0.925	0.032
21 (upper left central incisor)	0.91	0.013
22 (upper left lateral incisor)	0.959	0.275
23 (upper left canine)	0.91	0.013
31 (lower left central incisor)	0.95	0.152
32 (lower left lateral incisor)	0.943	0.098
33 (lower left canine)	0.957	0.246
41 (lower right central incisor)	0.978	0.745
42 (lower right lateral incisor)	0.978	0.755
43 (Lower right canine)	0.956	0.223

Table 4. Reliability test of consistency for reading by investigator by using paired t-test. In pairs column T indicates 1st digitization and B indicates 2nd digitization (n=5).

Pairs	Mean difference	Std. Deviation	95% CI		P-value
			Lower	Upper	
11T - 11B (upper right central incisor)	-1.24	2.48	-4.32	1.84	0.326
12T - 12B (upper right lateral incisor)	-1.16	1.84	-3.44	1.12	0.231
13T - 13B (upper right canine)	-0.3	2.14	-2.95	2.35	0.769
21T - 21B (upper left central incisor)	0.12	1.68	-1.97	2.21	0.881
22T - 22B (upper left lateral incisor)	-0.14	2.25	-2.94	2.66	0.896
23T - 23B (upper left canine)	0.3	1.87	-2.02	2.62	0.738
31T - 31B (lower left central incisor)	-0.3	2.61	-3.54	2.94	0.810
32T - 32B (lower left central incisor)	0.14	2.31	-2.73	3.01	0.899
33T - 33B (lower left canine)	0.62	4.17	-4.56	5.80	0.756
41T - 41B (lower right central incisor)	0.32	1.60	-1.66	2.30	0.677
42T - 42B (lower right lateral incisor)	0.14	2.48	-2.94	3.22	0.906
43T - 43B (lower right canine)	-0.36	2.71	-3.73	3.01	0.781

Table 5. Descriptive statistics of the MDBLAR per tooth (N=31).

Tooth	Mean	SD	Minimum	Median	Maximum	Skewness	Kurtosis
11 (upper right central incisor)	9.84	6.37	1	7.7	22.3	0.536	2.089
12 (upper right lateral incisor)	9.04	4.16	1.9	9.0	20.1	0.732	3.819
13 (upper right canine)	14.73	7.50	1.6	12.8	38.2	1.095	4.721
21 (upper left central incisor)	7.95	4.41	0.4	8.2	23.2	1.140	5.994
22 (upper left lateral incisor)	9.38	5.17	1.1	8.6	23.6	0.605	3.453
23 (upper left canine)	15.28	7.87	4.6	13.9	39.6	1.211	4.580
31 (lower left central incisor)	8.72	5.77	0.6	8.4	22.4	0.617	2.796
32 (lower left lateral incisor)	10.97	5.76	1	10.8	19.9	-0.112	1.710
33 (lower left canine)	11.68	5.12	3.5	11.0	26	0.653	3.479
41 (lower right central incisor)	8.78	4.47	0.1	8.6	16.9	0.001	2.100
42 (lower right lateral incisor)	10.76	4.67	2.1	10.3	19.9	0.098	2.268
43 (lower right canine)	10.45	5.39	0.4	10.1	20.9	-0.072	1.909

It should be noted that the maxillary central incisors and maxillary canines show higher evidence of non-normality. Figures 21-25 are plots illustrating histograms of the angles of these teeth. As expected from the skewness values, (most are positive) (Table 5) and from the nature of the data, the plots show a positive skew, with few values close to zero. The plots of the remaining teeth are almost normal, with the central plots at around 10 degrees.

Table 6, shows the comparison of MDBLAR between males and females. For almost all teeth there were no statistically significant differences in MDBLAR according to gender. The exception concerned the lower right central incisor, where the data showed a higher average of MDBLAR in males compared to females (P= 0.005).

With regard to teeth in which the MDBLAR was heterogeneous, no statistically significant differences were found between males and females in almost all teeth, except in the upper left central incisor where the median value was large in males compared to females (P= 0.022) (Table 7).

Tables8 and 9 show that there was no statistically significant difference in MDBLAR according to Angle classification.

Correlation between corresponding right and left teeth in the same arch were conducted to see if the angles of one tooth were related to the angles of another. Out of 6 correlations, the only significant statistic was found between upper right canine and upper left canine (r = 0.478, P = 0.007) (Table 10). Adjusting for multiple testing (Bonferroni) results in a P value of 0.05/6 = 0.008 and no statistically significant results. Therefore, it seems that angles of one tooth do not relate to angles of another.

Correlation between patients' age and angulation error showed that only upper right central and upper left canine values were correlated to patients' age, but P values were close to the 0.05 significance level and did not survive the Bonferroni adjustment.

Therefore, for the ages studied here, there was no effect of age on accuracy of root position estimation (Table 11).

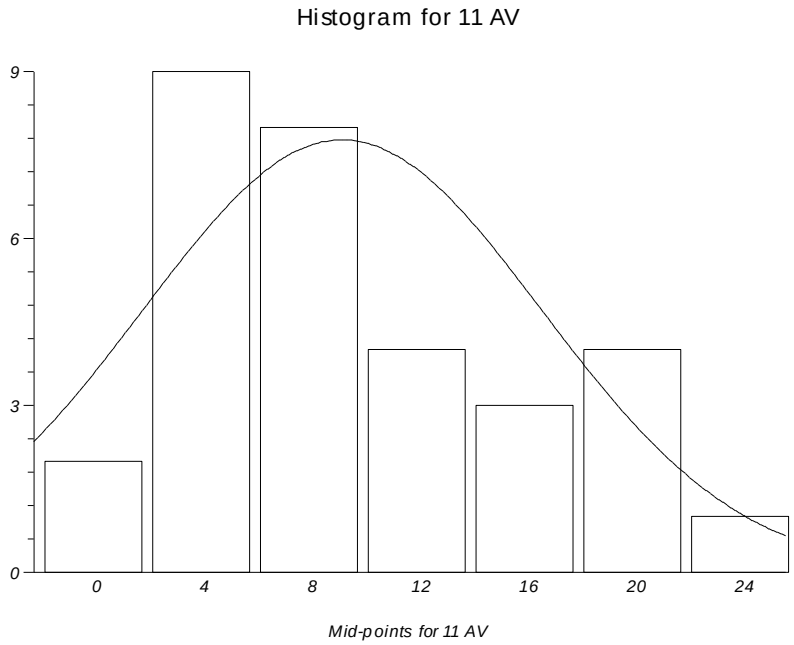

Figure 21. Plot illustrating histograms of the angles of upper right central incisor.

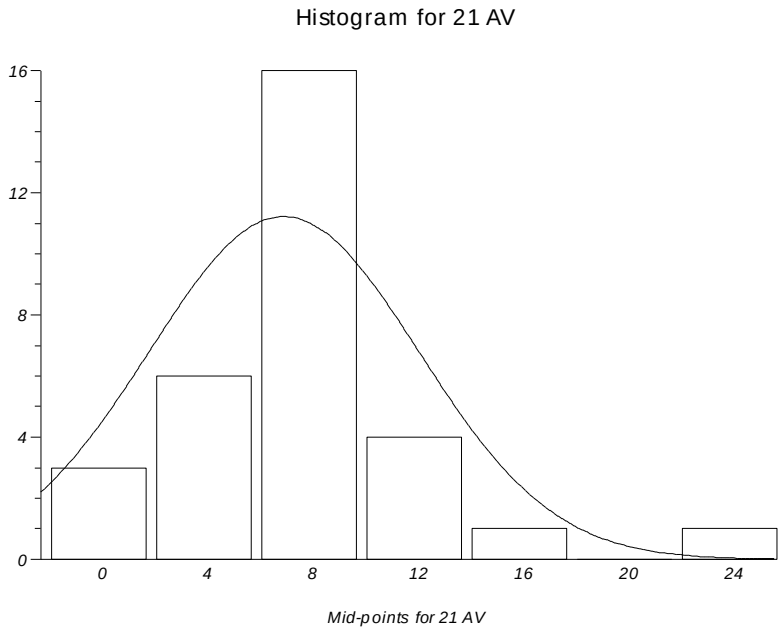

Figure 22. Plot illustrating histograms of the angles of upper left central incisor.

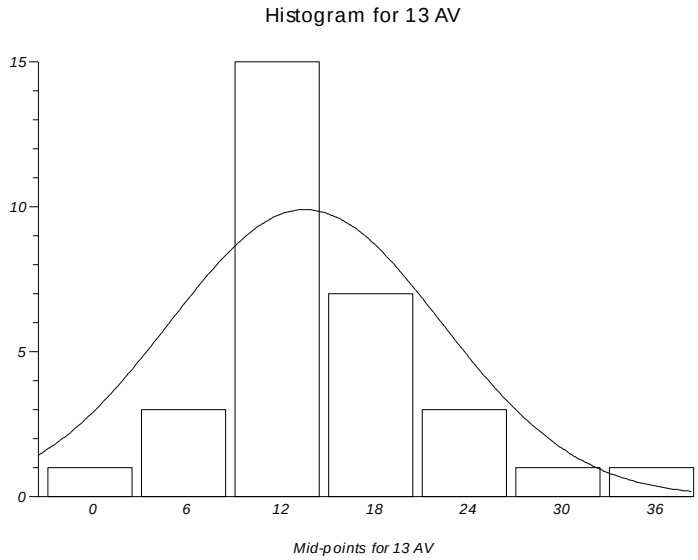

Figure 23. Plot illustrating histograms of the angles of upper right canine.

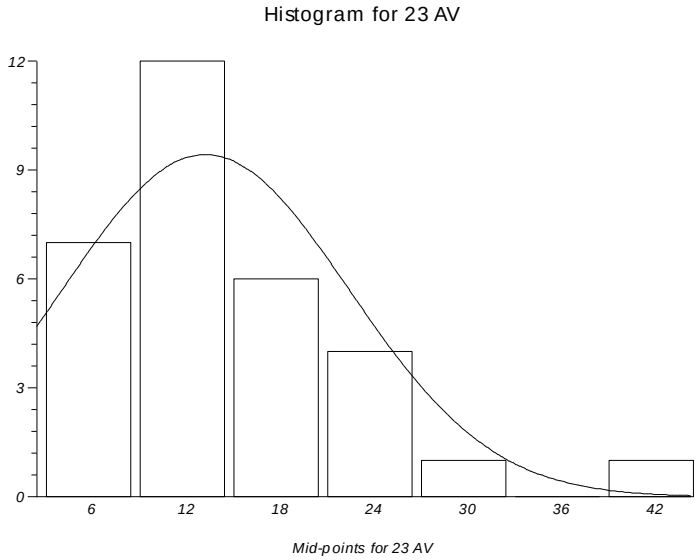

Figure 24. Plot illustrating histograms of the angles of upper left canine.

Table 6. Comparison of MDBLAR for each tooth per gender by t-test.

Tooth	Male mean(SD) N = 10	Female mean (SD) N = 21	P-value
12 (upper right lateral incisor)	7.99 (3.35)	9.53 (4.48)	0.343
22 (upper left lateral incisor)	10.54 (5.25)	6.94 (4.26)	0.069
31 (lower left central incisor)	9.20 (6.62)	7.69 (3.46)	0.410
32 (lower left lateral incisor)	11.88 (5.08)	9.08 (6.88)	0.212
33 (lower left canine)	12.66 (5.62)	9.82 (3.39)	0.166
41 (lower right central incisor)	10.26 (4.28)	5.68 (3.18)	0.005
42 (lower right lateral incisor)	10.72 (4.64)	10.84 (4.99)	0.950
43 (lower right canine)	10.01 (5.9)	11.38 (4.25)	0.519

Table 7. Comparison of MDBLAR by Mann-Whitney U test.

Tooth	Male Median (Min-Max) N = 10	Female Median(Min-Max) N = 21	P-value
11 (upper right central incisor)	12.5 [3.3 – 21.3]	7.3 [1 – 22.3]	0.173
13 (upper right canine)	14 [1.6 – 38.2]	12.8 [5.3 – 24.9]	0.724
21 (upper left central incisor)	9.5 [5.6 – 23.2]	7.3 [0.4 – 11.8]	0.022
23 (upper left canine)	15.2 [5.2 – 24.8]	13.2 [4.6 – 39.6]	0.416

Table 8. Using analysis of variance (ANOVA) to compare the MDBLAR per tooth within according to Angle classification.

Tooth	Angle Classification	N	Mean (SD)	P-value
12 (upper right lateral incisor)	Class I	5	11.72 (6.47)	0.059
	Class II div 1	17	7.6 (2.72)	
	Class II div 2	5	8.4 (2.88)	
	Class III	4	12.58 (5.07)	
22 (upper left lateral incisor)	Class I	5	10.86 (4.66)	0.265
	Class II div 1	17	10.48 (5.57)	
	Class II div 2	5	6.82 (2.97)	
	Class III	4	6.075 (5.05)	
31 (lower left central incisor)	Class I	5	9.32 (8.03)	0.507
	Class II div 1	17	9.53 (6.15)	
	Class II div 2	5	5.04 (3.54)	
	Class III	4	9.1 (1.41)	
32 (lower left lateral incisor)	Class I	5	8.74 (4.28)	0.085
	Class II div 1	17	13.08 (5.38)	
	Class II div 2	5	6.22 (5.10)	
	Class III	4	10.76 (6.87)	
33 (lower left canine)	Class I	5	10.42 (4.77)	0.172
	Class II div 1	17	13.49 (5.62)	
	Class II div 2	5	9 (3.14)	
	Class III	4	8.9 (2.54)	
41 (lower right central incisor)	Class I	5	10.12 (5.16)	0.515
	Class II div 1	17	9.25 (4.57)	
	Class II div 2	5	8.16 (2.97)	
	Class III	4	5.9 (5.04)	
42 (lower right lateral incisor)	Class I	5	8.38 (3.59)	0.492
	Class II div 1	17	11.4 (4.39)	
	Class II div 2	5	9.56 (7.40)	
	Class III	4	12.53 (2.66)	
43 (lower right canine)	Class I	5	9.76 (7.96)	0.801
	Class II div 1	17	10.5 (5.63)	
	Class II div 2	5	9.18 (3.74)	
	Class III	4	12.73 (2.88)	

Table 9. Using Kruskal Wallis test to compare the MDBLAR per tooth according to Angle classification.

Tooth	Angle Classification	N	Mean Rank	P-value
11 (upper right central incisor)	Class I	5	16.8	0.474
	Class II div 1	17	13.82	
	Class II div 2	5	19.2	
	Class III	4	20.25	
13 (upper right canine)	Class I	5	14.8	0.899
	Class II div 1	17	17.12	
	Class II div 2	5	14.9	
	Class III	4	14.13	
21 (upper left central incisor)	Class I	5	17.3	0.654
	Class II div 1	17	16	
	Class II div 2	5	12	
	Class III	4	19.38	
23 (upper left canine)	Class I	5	12.4	0.276
	Class II div 1	17	18.91	
	Class II div 2	5	12.3	
	Class III	4	12.75	

Table 10. Correlation coefficients between two corresponding teeth in the same arch.

Corresponding teeth	R in between	P-value
11 (upper right central incisor) 21 (upper left central incisor)	0.351	0.053
12 (upper right lateral incisor) 22 (upper left lateral incisor)	0.282	0.124
13 (upper right canine) 23 (upper left canine)	0.0478	0.007
31 (lower left central incisor) 41 (lower right central incisor)	0.207	0.263
32 (lower left lateral incisor) 42 (lower right lateral incisor)	0.165	0.376
33 (lower left canine) 43 (lower right canine)	0.149	0.424

Table 11. Correlation coefficients of age with each of the tooth angulation errors.

Tooth	R with Age	P-value
11 (upper right central incisor)	0.359	0.047
12 (upper right lateral incisor)	0.242	0.190
13 (upper right canine)	-0.310	0.090
21 (upper left central incisor)	-0.105	0.575
22 (upper left lateral incisor)	-0.149	0.424
23 (upper left canine)	-0.392	0.029
31 (lower left central incisor)	-0.005	0.977
32 (lower left lateral incisor)	-0.127	0.495
33 (lower left canine)	-0.348	0.055
41 (lower right central incisor)	-0.081	0.666
42 (lower right lateral incisor)	-0.050	0.788
43 (lower right canine)	-0.074	0.693

8. Discussion

Studies reported in the literature have shown that the use of digital models in the field of dentistry is growing rapidly (Keim et al., 2008, Martin et al., 2015). These studies confirmed that digital software is capable of faithfully reproducing dental structure with high degree of accuracy (Hirogaki et al., 2001). This development has been prompted by a range of perceived advantages including reduced storage requirement, rapid access to digital information, easy transfer of data and versatility (Hurt 2012).

To analyze the validity of root inclination prediction of digital models derived from Ortho Insight 3D scanner software, CBCT was chosen as a reference standard in this study. The introduction of dental CBCT has considerably expanded the scope of imaging and its use in the orthodontic clinical environment is rapidly expanding (Kapila et al., 2011). CBCT has proved to provide accurate measurements, with the 1-to-1 image-to-reality ratio making situations easy to understand (Lagravere et al., 2008).

No previous research appears to have been carried out on the accuracy and reliability of root inclination prediction derived from digital models that use a mathematical algorithm to produce an image of the anatomical roots using data gathered by digital scanning of the clinical crown.

In general, digital models have shown high degree of accuracy regarding tooth crown and dental arch reproduction. The hypothesis of this investigation was that there are differences in predicted root inclination characteristics generated by a commercially available 3D laser scanner software and the inclination characteristics derived from CBCT data.

It has been shown that linear anatomical measurements are not significantly different in digital models when compared to CBCT images when tooth crowns and dental arches were used as reference structures for measurements (Kau et al., 2010). Since no study has compared tooth root morphology characteristics between images from digital models and CBCT, it is a reasonable aim to carry out such an investigation by considering data from the latter process. From an ideal perspective, the real roots of normal teeth constitute the "gold standard" in terms of measurement. However, there are practical and ethical factors that make forming such a control group very difficult. Since the primary purpose of the commercially available software has been promoted and marketed as its usefulness in assessments and measurements derived from teeth crowns landmarks, the selection of the root inclination variable in this investigation was deliberately chosen as a key test of accuracy.

The variable of root inclination is simple to define, easy to understand and has meaningful orthodontic applications (e.g., evaluation of root parallelism before removal of fixed appliances).

Restricting evaluation to anterior teeth was chosen because a preliminary visual evaluation of digital models showed gross errors in the root imaging of posterior teeth (Figure 25), thus suggesting their exclusion from this study. In addition, anterior teeth are simpler in terms of morphology of both their crowns and roots.

The finding of this study showed a large range of discrepancies in the angle between the images derived from digital models and CBCT data, reaching almost 40 degrees in extreme cases (upper left canine). The canines showed the worst discrepancies, followed by the lower lateral incisors. The upper central incisors exhibit the best comparisons, although the maximum difference in angle exceeds 20 degrees (but the median was only around 8 degrees).

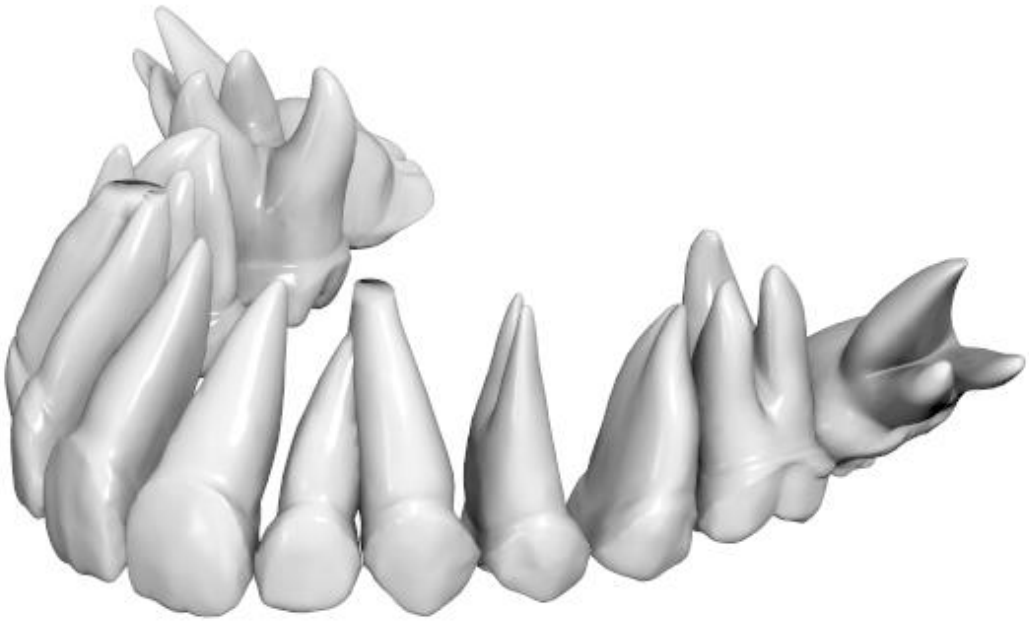

Figure 25. Original software estimation. Note overlapping of teeth 22 and 23 and gross errors of teeth 17 and 27.

It is evident from the data that significant errors are to be expected. In addition, the assessment of root inclination differences between images of digital models and CBCT data means that other important morphological features such as root length, volume, shape, were not included. Furthermore, the data from the results of this investigation does not indicate the direction of the angulation error, i.e. whether it was in mesio-distal or labio-lingual direction.

Errors of 10 degrees in estimating teeth mesio-distal or labio-lingual inclination should be considered as clinically notable. Figures 26 and 27 simulate this 10 degrees inclination and illustrate significant overlapping of adjacent roots, which is not clinically possible unless there is extensive root resorption or excessive variation in root shape.

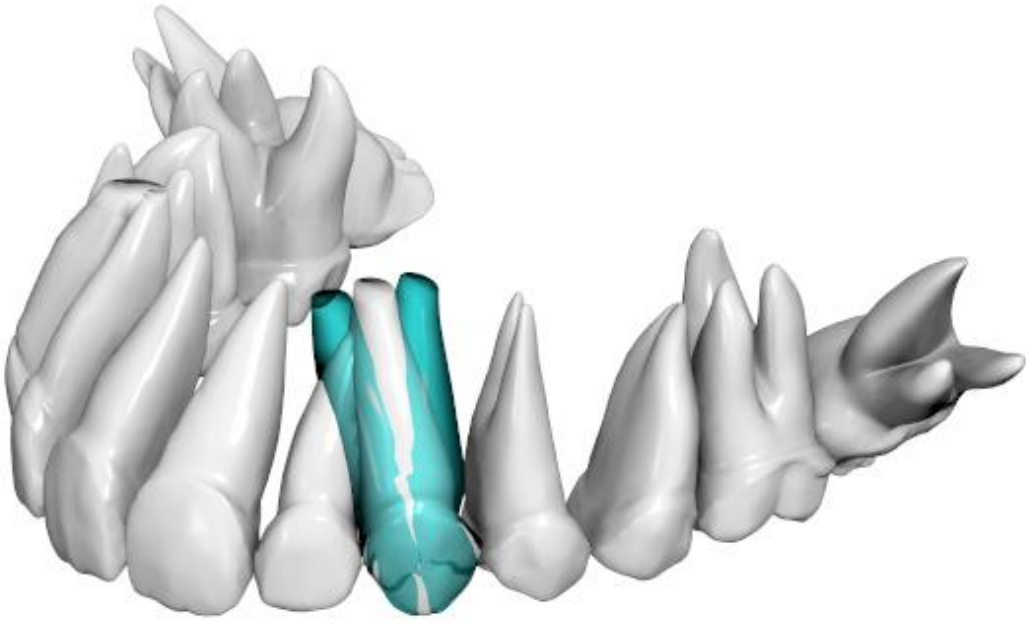

Figure 26. Ten degree tipping on either side of upper left canine.

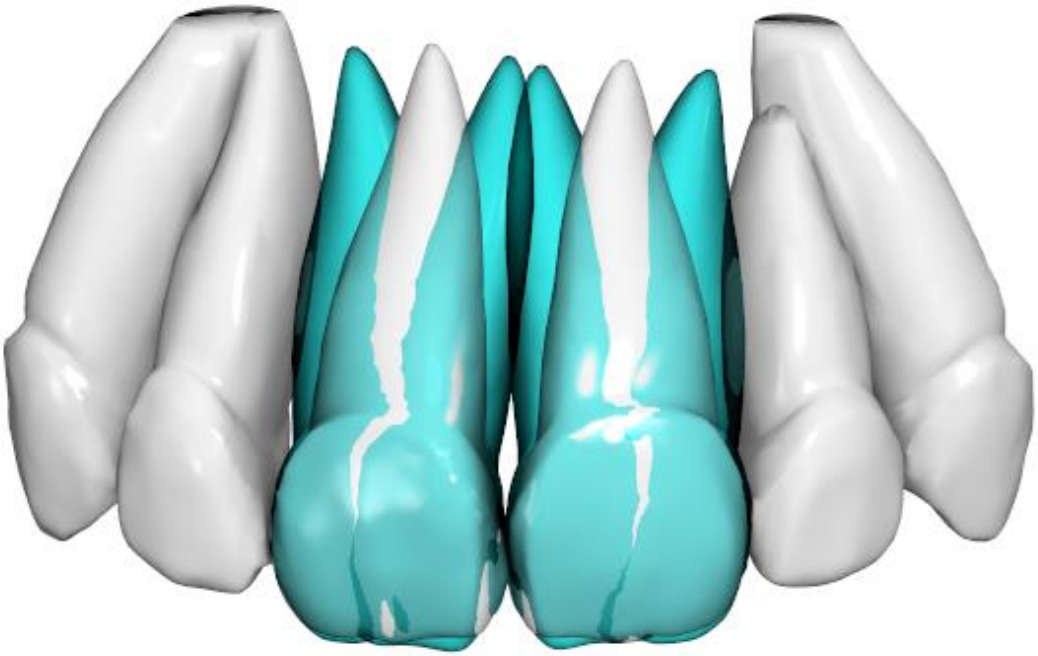

Figure 27. Ten degree tipping on either side of upper central incisors.

Previous studies using CBCT have demonstrated high degrees of accuracy and reliability in measurements of root length and root shortening when CBCT images were compared to direct skull measurements of teeth (Lund et al., 2010) and to periapical radiographs (Sherrard et al., 2010).

The commercially available software which has been used in this investigation, has received excellent reviews regarding its use in providing dental arch measurements as well as in performing space analyses, tooth size discrepancy evaluation and other orthodontic applications based on landmarks derived from tooth crown morphology (Bailey et al., 2013). Sensitivity of methodology, for example superimposition of teeth crowns of CBCT image and digital model is one of the limitations of this project. Root morphology imaging prediction is not a function that this software has been designed to provide and this study verifies its limitation in routine clinical applications when used alone. However, simulation of root morphology based on scanning of plaster dental models, or dental impressions is an initial additional step, which would prove very advantageous in the future, if the accuracy of the prediction can be significantly improved.

However, at the present time, these predictions cannot be considered accurate and reliable unless they are correlated with a radiographic image. If this kind of software could be given the ability to predict all the required criteria available for evaluation in a radiograph, without the need to expose the patient to radiation, it would provide significant clinical benefits.

9. Conclusions

This investigation was carried out to test the hypothesis that there are differences in predicted anterior teeth root inclination characteristics generated by commercially available 3D laser scanner software and the inclination characteristics derived from CBCT data. The research hypothesis was verified because notably different anterior teeth root inclinations between the two images have been clearly demonstrated.

The results of the study lead to the following conclusions:

1- A median value for the angle between true root position derived from CBCT and estimated position ranging from 7.7 t0 13.9 degrees was found, but errors of more than 20 degrees are not uncommon.

2- Visual observation of the cases showed that the software frequently estimates angulations that lead to overlapping of adjacent roots, a clinically impossible situation unless there is extensive root resorption or root morphology variation.

3- Errors are higher for upper and lower canines and lower for upper and lower central incisors.

4- No differences were found in the inclination between true root position derived from CBCT and estimated position among different Angle classifications.

5- No differences were found in the inclination between true root position derived from CBCT and estimated position in almost all variables between the different gender and age groups.

6- There is no correlation of errors between teeth. This implies that the software probably evaluates each tooth individually. This is confirmed by the overlapping of roots mentioned above.

10. References

Agustín-Panadero R, Peñarrocha-Oltra D, Gomar-Vercher S, Ferreiroa A, Peñarrocha-Diago M. Implant-supported overdenture manufactured using CAD/CAM techniques to achieve horizontal path insertion between the primary and secondary structure: A clinical case report. J Adv Prosthodont 2015;7:264–270.

Akyalcin S, Dyer DJ, English JD, Sar C. Comparison of 3-dimensional dental models from different sources: diagnostic accuracy and surface registration analysis. Am J Orthod Dentofacial Orthop 2013;144:831-7.

Anusavice KJ. Phillips' Science of Dental Materials. Philadelphia, Saunders, 2003.

Aragón ML, Pontes LF, Bichara LM, Flores Mir C, Normando D. Validity and reliability of intraoral scanners compare to conventional gypsum models measurements: a systemic review. Eur J Orthod 2016 June 7,pii: cjw033.[Epub ahead of print].

Assadian H, Dabbaghi A, Gooran M, Eftekhar B, Sharifi S, Shams N, Dehghani Najvani A, Tabesh H. Accuracy of CBCT, digital radiography and cross-sectioning for the evaluation of mandibular incisor root canals. Iran Endod J 2016;11:106-10.

Axelsson P. Processing of laser scanner data-algorithms and applications. J Photogrammetry Remote Sensing 1999;54:138-47.

Bailey E, Nelson G, Miller AJ, Andrews L, Johnson E. Predicting tooth-size discrepancy: a new formula utilizing revised landmarks and 3-dimensional laser scanning technology. Am J Orthod Dentofac Orthop 2013;143:574-85.

Bell GW, Rodgers JM, Grime RJ, Edwards KL, Hahn MR, Dorman ML, Keen WD, Stewart DJ, Hampton N. The accuracy of dental panoramic tomographs in determining the root morphology of mandibular third molar teeth before surgery. Oral Surg Oral Med Oral Pathol Oral Radiol Endod 2003;95:119-25.

Benninger B, Peterson A, Cook V. Assessing validity of actual tooth height and width from cone beam images of cadavers with subsequent dissection to aid oral surgery. J Oral Maxillofac Surg 2012;70:302-6.

Besl PJ, McKay ND. A method for registration of 3-D shapes. IEEE Trans on Pattern Analysis and Machine Intelligence 1992;14:239-56.

Birnbaum N, Aaronson HB, Stevens C, Cohen B. 3D digital scanners: a high-tech approach to more accurate dental impression. Inside Dentistry 2009;5:70-4.

Brezden NA, Brooks SL. Evaluation of panoramic dental radiographs taken in private practice. Oral Surg Oral Med Oral Pathol 1987;63:617-21.

Brons S, Beusichem ME, Bronkhorst EM, Draaisma J, Bergé SJ, Maal TJ, Kuijpers-Jagtman AM. Methods to quantify soft-tissue based facial growth and treatment outcomes in children: a systematic review. PLoS One 2012;7:e41898.

Cho PS, Johnson RH, Griffin TW. Cone-beam CT for radiotherapy applications. Phys Med Biol 1995;40:1863-83.

Christensen GJ. Impression are changing: deciding on conventional, digital or digital plus in-office. J Am Dent Assoc 2009;140:1301-4.

El-Angbawi AMF, McIntyre GT, Bearn DR, Thomson DJ.Film and digital periapical radiographs for the measurement of apical root shortening. J Clin Exp Dent 2012;4: e281-e5.

Farman AG, Farman TT. Extraoral and panoramic systems. Dent Clin North Am 2000;257-72.

Farman TT, Farman AG. Clinical trial of panoramic dental radiography using a CCD receptor. J Digit Imaging 1998;11:169-71.

Flores-Mir C, Rosenblatt MR, Major PW, Carey JP, Heo G. Measurement accuracy and reliability of tooth length on conventional and CBCT reconstructed panoramic radiographs. J Orthod 2014;19:45-53.

Germec-Cakan D, Canter HI, Nur B, Arun T. Comparison of facial soft tissue measurements on three-dimensional images and models obtained with different methods. J Craniofac Surg 2010;21:1393-9.

Gijbels F, De Meyer AM, Bouserhal J, Van den Bossche C, Declerck J, Persoons M, Jacobs R. The subjective image quality of direct digital and conventional panoramic radiography. Clin Oral Invest 2000;4:162-7.

Glenner RA. Dental impressions. J Hist Dent 1997;45:127-30.

Grünheid T, Patel N, De Felippe NL, Wey A, Gaillard PR, Larson BE. Accuracy, reproducibility, and time efficiency of dental measurements using different technologies. Am J Orthod Dentofacial Orthop 2014;145:157-64.

Hajeer MY, Millett DT, Ayoub AF, Siebert JP. Applications of 3D imaging in orthodontics: part I. J Orthod 2004;31:62-70.

Han UK, Vig KW, Weintraub JA, Vig PS, Kowalski CJ. Consistency of orthodontic treatment decisions relative to diagnostic records. Am J Orthod Dentofac Orthop 1991;100:212-219.

Hatcher DC. Operational principles for cone-beam computed tomography. J Am Dent Assoc 2010;141:3S-6S.

Hillson S. Dental Anthropology. Cambridge, Cambridge University Press, 1996.

Hirogaki Y, Sohmura T, Satoh H, Takahashi J, Takada K. Complete 3-D reconstruction of dental case shape using perceptual grouping. IEEE Trans Med Imaging 2001;20:1093-101.

Hollenbeck K, Allin T, Poel M. Dental Lab 3D Scanners–How they work and what works best. Copenhagen, 3Shape Technology Research, 2012.

Horton HM, Miller JR, Gaillard PR, Larson BE. Technique comparison for efficient orthodontic tooth measurements using digital models. Angle Orthod. 2010;80:254-61.

Hurt AJ. Digital technology in the orthodontic laboratory. Am J Orthod Dentofacial Orthop 2012;141:245-7.

Issacson KG, Thom AR, Atack NE, Horner K, Whaites E. Orthodontic Radiographs - Guidelines. London, British Orthodontic Society, 2015:22-24.

Jeong ID, Lee JJ, Leon JH, Kim JH, Kim WC. Accuracy of complete-arch model using an intraoral video scanner: An in vitro study. J Prosthet Dent 2016;115:755-9.

Jiang T, Lee SM, Hou Y, Chang X, Hwang H. Evaluation of digital dental models obtained from dental cone-beam computed tomography scan of alginate impressions. Korean J Orthod 2016;46:129-136.

Kapila S, Conley RS, Harrell WE Jr. The current status of cone-beam computed tompgraphy imaging in orthodontics. Dentofac Radiol 2011;40:24-34.

Kapila S, Farman AG. Craniofacial imaging in the 21st century. Proceedings of the 2002 COAST Conference, California. Orthod Craniofac Res 2003;6:7-8.

Kapila SD, Nervina JM. CBCT in orthodontics: assessment of treatment outcomes and indications for its use. Dentomaxillofac Radiol 2015;44:201-8.

Kaeppler G, Axmann-Kecmar D, Reuter I, Meyle J, Gomez-Roman G. A clinical evaluation of some factors affecting image quality in panoramic radiography. Dentomaxillifac Radiol 2000;29:81-4.

Kamtane S, Ghodke M. Morphology of mandibular incisors: A study on CBCT. Pol J Radiol 2016;81:15-6.

Kau CH, Littlefield J, Rainy N, Nguyen JT, Creed B. Evaluation of CBCT digital models and traditional models using little's index. Angle Orthod 2010;80:345-9.

Keim RG, Gottlieb EL, Nelson AH, Vogels DS. Study of orthodontic diagnosis and treatment procedure, part 1: Results and trends. J Clin Orthod 2008;42:625-40.

Kim SY, Kim MJ, Han JS, Yeo IS, Lin YJ, Kwan HB. Accuracy of dies captured by an intraoral digital impression system using parallel confocal imaging. Int J Prosthod 2013; 26;161-3.

Kochel J, Meyer-Marcotty P, Strnad F, Kochel M, Stellzig-Eisenhauer A. 3D soft tissue analysis - part 1: sagittal parameters. J Orofac Orthop 2010;71:40-52.

Kravitz ND, Groth C, Jones PE, Graham JW, Redmond WR. Intraoral digital scanners. J Clin Orthod 2014;48:337-47.

Lagravere MO, Carey J, Toogood RW, Major PW. Three dimensional accuracy of measurement made with software of cone-beam computed tomography images. Am J Ortho Dentofacial Orthop 2008;134:112-6.

Lee RJ, Weissheimer A, Pham J, Go L, Menezes LM, Redmond WR, Loos JF, Sameshima GT, Tong H. Three-dimensional monitoring of root movement during orthodontic treatment. Am J Orthod Dentifacial Orthop 2015; 147: 132-42.

Leifert MF, Leifert MM, Efstratiadis SS, Cangialosi TJ. Comparison of space analysis evaluation with digital models and plaster dental casts. Am J Orthod Dentofacial Orthop 2009;136:1-4.

Lestrel PE. Some approches toward the mathematical modeling of the craniofacial complex. J Craniofac Genet Dev Biol 1989;9:77-91.

Littlefield TR, Kelly KM, Cherney JC, Beals SP, Pomatto JK. Development of a new three-dimensional cranial imaging system. J Craniofac Surg 2004;15:175-81.

Lübbers HT, Medinger L, Kruse A, Grätz KW, Matthews F. Precision and accuracy of the 3dMD photogrammetric system in craniomaxillofacial application. J Craniofac Surg 2010;21:763-7.

Lund H, Gröndahl K, Gröndahl HG. Cone beam computed tomography for assessment of root length and marginal bone level during orthodontic treatment. Angle Orthod 2010;80:466-73.

Mah JK. The cutting edge. J Clin Orthod 2003;37:101-3.

Mah JK, Huang JC, Choo H. Practical application of cone beam computed tomography in orthodontics. J Am Dent Assoc 2010;141:7S-13S.

Maroua Al, Ajaj M, Hajeer MY. Accuracy and reproducibility of linear measurements made on CBCT-derived digital models. J Contemp Dent Pract 2016;17:294-9.

Martin CB, Chalmers EV, McIntyre GT, Cochrane H, Mossey PA. Orthodontic scanners: what is available? J Orthod 2015;42:136-43.

Melsen B, Agerbæk N, Markenstam G. Intrusion of incisors in adult patients with marginal bone loss. Am J Orthod Dentofac Orthop 1989;96:232-41.

Mokhtari H, Niknami M, Mokhtari Zonouzi HR, Sohrabi A, Ghasemi N, Akbari Golzar A. Accuracy of Cone-Beam Computed Tomography in determining the root canal morphology of mandibular first molars. Iran Endod J 2016;11:101-5.

Mörmann WH. The evolution of the CEREC system. J Am Dent Assoc 2006;137;7S-13S.

Mörmann W, Brandestini M, Ferru A, Lutuz F, Krejci I. Marginal adaptation of camera. Int J Comput Dent 1985;12:11-28.

Mörmann WH, Brandestini M, Lutz F, Barbakow F. Chairside computer-aided direct ceramic inlays. Quintessence Int 1989;20:329-39.

Moze G, Seehra J, Fanshawe T, Davies J, McDonald F, Bister D. In vitro comparison of contemporary radiographic imaging techniques for measurement of tooth length: reliability and radiation dose. J Orthod 2013;40:225-33.

Mozzo P, Procacci C, Tacconi A, Martini PT, Andreis IA. A new volumetric CT machine for dental imaging based on the cone-beam technique: preliminary results. Eur Radiol 1998;8:1558-64.

Mullen SR, Martin CA, Ngan P, Gladwin M. Accuracy of space analysis with emodels and plaster models. Am J Orthod Dentofacial Orthop 2007;132:346-52.

Naidu D, Scott J, Ong D, Ho CT. Validity, reliability and reproducibility of three methods used to measure tooth widths for Bolton analyses. Aust Orthod J 2009;25:97-103.

Nakajima A, Murata M, Tanaka E, Arai Y, Fukase Y, Nishi Y, Sameshima G, Shimizu N. Development of three-dimensional FE modelling system from the limited cone beam CT images for orthodontic tipping tooth movement. Dent Mater J 2007;26:882-91.

Ning R, Chen B. Cone beam volume CT breast imaging: feasibility study. Med Phys 2002; 29:755-70.

Peluso MJ, Josell SD, Levine SW, Lorei BJ. Digital models: an introduction. Semin Orthod 2004;10:226-38.

Persson A, Andersson M, Oden A, Sandborgh-Englund G. A three-dimensional evaluation of a laser scanner and a touch-probe scanner. J Prosthet Dent 2006;96:194-200.

Pepelassi EA, Tsiklakis K, Diamanti-Kipioti A. Radiographic detection and assessment of the periodontal defects. J Clin Periodontol 2000;27:224-30.

Qiao J, Duan JY, Sun CZ, Liu DG. Accuracy analysis of cone beam computed tomography in assessing furcation involvements of mandibular molars. Beijing Da Xue Xue Bao 2014;46:975-9.

Read DW, Lestrel PE. A comment upon uses of homologous-point measures in systematic: a reply to Brookstein et al. Syst Zool 1986;35:241-53.

Robb RA. Dynamic spatial reconstruction: An X-ray video fluoroscopic CT scanner for dynamic volume imaging of moving organs. IEEE Trans Med Imag 1982;1:22-3.

Rose JC, Condon KW, Goodman Ah. Diet and dentition: Developmental disturbances. In: Gilbert RI, Jr., Meilke JH, eds. The Analysis of Prehistoric Diets. Orlando, Academic Press 1985;281-305.

Rushton VE, Horner K, Worthington HV. The quality of panoramic radiographs in a sample of general dental practices. Br Dent J 1999;186:630-3.

Russell M. Destroying patient records. California Association of Orthodontists Website, 2002.

Scarfe WC, Farman AG. What is Cone-Beam CT and how does it work? Dent Clin N Am 2008;52:707-30.

Schaefer O, Kuepper H, Sigusch BW, Thompson GA, Hefti AF, Guentsch A. Three-dimensional fit of lithium disilicate partial crowns in vitro. J Dent 2013,41:271-7.

Scott Gr, Turner CG. The Anthropology of Modern Human Teeth. Cambridge, Cambridge University Press, 1997.

Sherrard JF, Rossouw PE, Benson BW, Carrillo R, Buschang PH. Accuracy and reliability of tooth and root lengths measured on cone-beam computed tomographs. Am J Orthod Dentofacial Orthop 2010;137:S100-8.

Silva MA, Wolf F, Heincke BU, Mann Visser H. Cone beam computer tomography for routine orthodontic treatment planning a radiation dose evaluation. Am J Orthod Dentofac Orthop 2008;133:640;e1-5.

Stewart MB. Dental models in 3D. Orthod Prod 2001;21-4.

Syriopoulos K, Sanderink GC, Velders XL, Van der Stelt PF. Radiographic detection of approximal caries: a comparison of dental films and digital imaging systems. Dentomaxillofac Radiol 2000;29:312-8.

Ting-Shu S, Jian S. Intraoral digital impression technique: a review. J Prosthod 2015;24:313-21.

Villarrubia JS. Algorithms for scanned probe microscope image simulation, surface reconstruction, and tip estimation. J Res Natl Inst Stand Technol 1997;102:425-54.

Weber MT, Stratz N, Fleiner J, Schulze D, Hannig C. Possibilities and limits of imaging endodontic structures with CBCT. Swiss Dent J 2015;125:293-311.

Whaites E, Drage N. Essentials of Oral Radiography and Radiology. London, Churchill Livingstone, 2013.

Witcher TP, Brand S, Gwilliam JR, McDonald F. Assessment of the anterior maxilla in orthodontic patients using upper anterior occlusal radiographs and dental panoramic tomography: a comparison. Oral Surg Oral Med Oral Pathol Oral Radiol Endod 2010;109:765-74.

Yang YQ, Mi ZL, Ge ZL. Comparison between the tooth length measured by cone-beam CT and the tooth length measured with Vernier calliper. Zhonghua Kou Qiang Yi Xue Za Zhi 2013;48:689-93.